DOCTRAL THESIS

（博士学位論文）

Development of Air Bubble-Mediated Separation and Purification Methods

（気泡を用いる分離・精製技術の開発）

Author

Koki KODAMA

（児玉　康輝）

KITAMI INSTITUTE OF TECHNOLOGY

GRADUATE SCHOOL OF ENGINEERING

March 2024

CONTENTS

ABSTRACT

It was found that the air-water interface (air-bubbles) could be used as a separation medium for the purification of dyes and pharmaceuticals. Air bubbles are a harmless, waste-free medium with a low environmental impact. This study suggests that the air-water interface has solvent properties comparable to those of ethyl acetate and is effective in the purification of the basic dye Rhodamine B and the anti-malarial drug Chloroquine, providing the basis for a possible new method of compounds separation and purification.

In Chapter 2, the hydrophobic properties of bubbles as separation media were clarified by analysis using fluorescent probes and ultrafine bubbles (UFB), which are stable in water. Measurements using the fluorescent molecule 1,2'-dinaphthylamine, which is used to evaluate hydrophobic field, observed that water containing UFB is a much more hydrophobic solvent than water. The hydrophobicity of the bubbles was similar to that of ethyl acetate and diethyl ether, indicating the characteristics of bubbles as separation media.

Chapter 3 shows a rapid purification method for chloroquine based on flotation. Chloroquine, an antimalarial drug, is synthesized in about 80% yield by 4-amino-1diethylaminopentane and 4,7-dichloroquinoline. It has been purified by solvent extraction and then recrystallization. The method designed utilizes the differences in hydrophobicity and ionicity between the source material and the product, achieving a rapid separation in less than 10 minutes. The purity of the product was more than 99% by HPLC analysis. The use of bubbles as a separation medium has been shown to provide low environmental impact pharmaceuticals purification.

Chapter 4 was a fundamental study for industrial continuous treatment combined with microfiltration (MF). MF membranes have the advantage of good permeability and

resistance to fouling, but their large pore size prevents them from blocking low molecular compounds such as dyes. We found that a specific dye can be blocked by passing a solution containing bubbles larger than the membrane pore size through an MF membrane, taking advantage of the properties of bubbles.

Air-bubbles as a separation medium were found to have solvent properties similar to ethyl acetate and could rapidly adsorb and separate compounds with strong hydrophobic properties. it is even possible to prevent the permeation of compounds into the microfiltration membrane by means of adsorption of molecules on the bubbles. It is hoped that this research will provide the beginnings of a new low environmental impact separation method that could contribute to a sustainable society.

ABSTRACT IN JAPANESE

気液界面（気泡）が分離媒体として色素や医薬品の精製に利用できる可能性が見出された。空気からなる気泡は無害で廃棄物の発生しない低環境負荷な媒体である。本研究により、気液界面は酢酸エチルと同程度の溶媒特性を有していることが示唆され、塩基性色素ローダミン B や抗マラリア薬クロロキンの精製に有効であることが判明し、新しい物質分離・精製法となり得る端緒が見出された。

第 2 章では分離媒体として観た気泡の持つ疎水的な性質について、蛍光プローブと水中でも安定なウルトラファインバブル(UFB)を用いた分析によって明らかにさせた。疎水的な環境評価に用いられる蛍光分子 1,2'-ジナフチルアミンを用いた測定によって、UFB 含有水が水と比べてはるかに疎水的な溶媒であることが観察された。その疎水的な性質は酢酸エチルやジエチルエーテルに近いという結果が得られ、分離媒体として観た気泡の特性が明らかになった。

第 3 章に浮選を基にしたクロロキンの迅速精製法を示した。抗マラリア薬であるクロロキンは 4-アミノ-1-ジエチルアミノペンタンと 4,7-ジクロロキノリンにより 8 割の収率で合成され、溶媒抽出と再結晶を経て精製されている。考案した手法は原料物質と生成物との疎水性やイオン性の違いを利用し、10 分未満と速やかな分離に成功した。生成物の純度は HPLC の分析にて 99%以上を達成できた。気泡を分離媒体とすることで、低環境負荷な物質精製が可能であることが示された。

第 4 章は精密ろ過(MF)との組み合わせにより、工業的な連続処理を見据えた基礎検討を行った。MF 膜は通水性が良く、目詰まりしにくいという利点があるが、その孔径ゆえに色素など低分子化合物を阻止できない。我々は気泡の性質を利用し、膜孔径より大きな気泡を含む溶液を MF 膜に通すことで、特定色素を透過阻止できることを発見した。

分離媒体としての気泡は酢酸エチルに近い溶媒特性を持ち、疎水性の強い化合物を速やかに吸着、分離できることが判明した。また、気泡への物質吸着を利用することで、精密ろ過膜への分子の透過を阻止することさえ可能である。本研究により、低環境負荷な新しい分離法の端緒が見出され、持続可能な社会実現への一助となり得ることが期待される。

List of Figures

CHAPTER 1
INTRODUCTION

In the chemical industry, there is a need to develop methods that are rapid, cost effective and have a lower environmental impact in order to achieve a sustainable society. This Started with the proposal of Green Chemistry in 1998[1,2]. Following the adoption of the Sustainable Development Goals (SDGs) by the UN General Assembly in 2015[3], it is predicted that industry will need to develop processes that take those objectives into account even more in the future. Chemical manufacturing processes are broadly divided into synthesis and separation-purification, with separation dominated by traditional methods and not undergoing innovative changes. For example, crystallization, solid phase extraction and solvent extraction are separation methods that have long been used industrially[4]. However, crystallization is time-consuming and requires several hours of processing time[5,6]. The latter two has the problem of using a large amount of environmentally hazardous organic solvents as separation media[7,8]. Recently, ionic liquids (including deep eutectic solvents) [9-15], critical fluids[16-20], and membrane filtration[21,22] have attracted attention as separation media for green chemistry. Ionic liquids raise concerns about potential environmental toxicity[23], and critical fluids and membrane filtration are expensive to install and operate. Therefore, it is important for the next generation of the chemical industry to develop innovative rapid separation and purification technologies using environmentally friendly and inexpensive separation media.

To solve this issue, we have investigated using bubbles (air-water interface) as a separation medium. Bubbles are an ideal media because they are easy to generate, harmless and waste-free. In addition, rapid and low-cost process development seems possible, as demonstrated by foam separation [24-27], a typical bubble-based separation

method. It has been observed that bubbles in water can attract hydrophobic or amphiphilic solute molecules. This is because non-polar molecules are thermodynamically more stable if hydration is avoided as far as possible. The absence of water molecules at the air-water interface causes non-polar molecules to be attracted to the bubbles as if they were adsorbing on them. Hence, it has been predicted that bubbles as separation media will act as a kind of organic solvent, trapping hydrophobic molecules in the water, but the details have not been clarified. For the further development of separation methods using bubbles, it is important to understand the specific hydrophobicity of bubbles and to clarify the solvent properties of bubbles as a separation medium.

Previously, we successfully developed a surfactant-free flotation process[27] specifically for dye purification. A flotation[28,29] is a type of foam separation and is known as a rapid process using air bubbles. However, the conventional flotation[28, 30-33] lacks selectivity and requires a collector such as a bubble modified with a surfactant or an organic solvent in the separation medium, making it difficult to apply the method to purification where only a single compound is separated. We have developed the flotation method[24] that is highly selective and does not require collectors such as surfactants. The method is illustrated in Fig.1-1. It requires only 0.1 ml of ethanol, which is a harmless compound, and the processing time is as short as 10 minutes, making it effective in solving the aforementioned problems. By clarifying the characteristics of bubbles as a separation medium, which is the key to this method, and discussing the applicability to other compounds and the practicality of industrialization, it is possible to establish a new separation method that is inexpensive, rapid, and has a low environmental impact.

In this study, we evaluated the solvent properties of bubbles as a separation medium and clarified the chemistry of the air-water interface. The resulting knowledge was applied to the purification of pharmaceuticals, an important

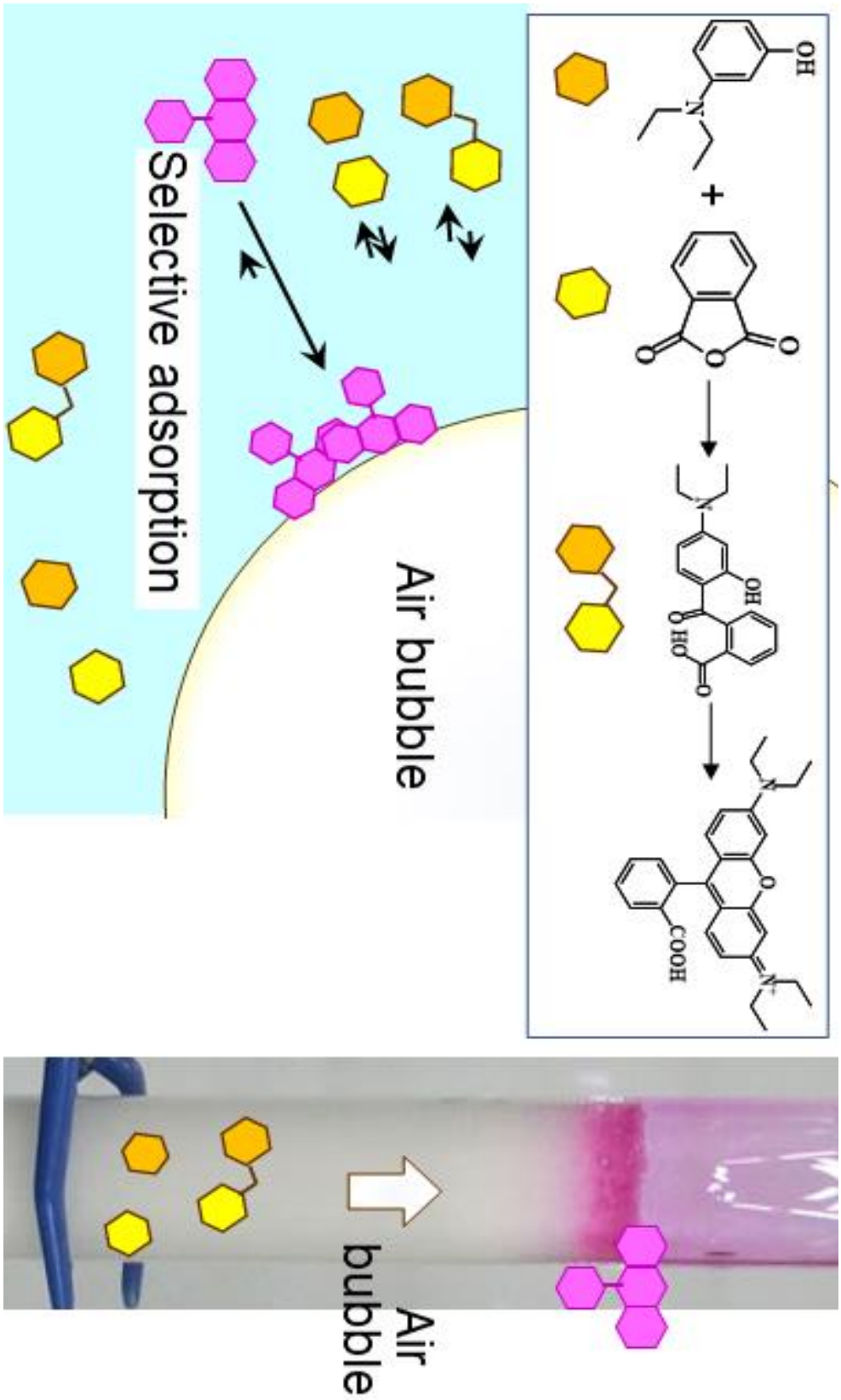

Fig.1-1 Surfactant-free and selective flotation.

group of chemical products. In addition, a separation method combining bubbles and microfiltration was investigated for industrial applicability and even more rapid separation.

In Chapter 2, the solvent properties of bubbles were evaluated using a fluorescent probe, and the microscopic properties of bubbles as a separation medium were discussed. In Chapter 3, we focused on chloroquine, a pharmaceutical known as an anti-malarial drug, and examined a purification method by surfactant-free flotation. Through these studies, the mechanism of the separation method using bubbles was clarified. In Chapter 4, we explored the possibility of exploiting the properties of bubbles and combining them with microfiltration to further increase speed and continuous processing. Finally, air bubble-mediated separation and purification technologies were discussed in Chapter 5.

References.

[1]. P. T. Anastas, "Green Chemistry" Theory and Practice, 1998.

[2]. J. H. Clark, Green chemistry: challenges and opportunities, Green Chemistry, **1**, 1-8(1999).

[3]. United Nations, Transforming our world: the 2030 Agenda for Sustainable Development, 2015. <https://www.unic.or.jp/activities/economic_social_development/sustainable_development/2030agenda/>.

[4]. N. G. Anderson, Practical Process Research & Development: A guide for organic chemists Second Edition, 2012.

[5]. Y. Yang, K. Pal, A. Koswara, Q. Sun, Y. Zhang, J. Quon, R. McKeown, C. Goss, Z. K. Nagy, Application of feedback control and in situ milling to improve particle size and shape in the crystallization of a slow growing needle-like active pharmaceutical ingredient *Int. J. Pharmaceut.*, **533***,* 49-61(2017).

[6]. D. Zhang, S. Xua, S. Dua, J. Wang, J. Gong, Progress of Pharmaceutical Continuous Crystallization, Engineering, **3**, 354-364 (2017).

[7]. B. Schuur, T. Brouwer, D. Smink, L. M. J. Sprakel, Green solvents for sustainable separation processes, *Curr. Opin. Green. Sustain. Chem.*, **18**, 57-65 (2019).

[8]. M. C. Bubalo, S. Vidovic, I. R. Redovnikovic, S. Joki., Green solvents for green technologies, *J. Chem. Technol. Biotechnol.*, **90**, 1631-1639(2015).

[9]. S. Werner, M. Haumann, Ionic liquids in chemical engineering, *Annu. Rev. Chem. Biomol. Eng.*, **1**, 203-230 (2010).

[10]. I. M. Marrucho, L. C. Branco, L. P. N. Rebelo, Ionic Liquids in Pharmaceutical Applications, *Annu. Rev. Chem. Biomol. Eng.,* **5**, 527-546 (2014).

[11]. A. P. de los. Rios, A. Irabien, F. Hollmann, F. J. H. Fernandez, Ionic liquids: Green solvents for chemical processing, Journal of Chemistry, 2013(2013).

[12]. Y. H. Choi, R. Verpoorte, Green solvents for the extraction of bioactive compounds from natural products using ionic liquids and deep eutectic solvents, *Curr. Opin. Food Sci.*, **26**, 87-93 (2019).

[13]. A. S. Dheyab, M. F. A. Baker, M. Alomar, S. F. Sabran, A. F. M. Hanafi, A. Mohamad, Deep eutectic solvents (DESs) as green extraction media of beneficial bioactive phytochemicals, *Separations*, **8**, 10, 176 (2021).

[14]. H. Balaraman, R. Selvasembian, V. Rangarajan, S. Rathnasamy, Sustainable and Green Engineering Insights on Deep Eutectic Solvents toward the Extraction of Nutraceuticals, *ACS Sustain. Chem. Eng.,* **9**, 34, 11290-11313 (2021).

[15]. P. Makoś, A. Przyjazny, G. Boczkaj, Hydrophobic deep eutectic solvents as "green" extraction media for polycyclic aromatic hydrocarbons in aqueous samples, *J. Chromatogr. A*, **5,** 1570, 28-37 (2018).

[16]. M. M. R. de Melo, A. J. D. Silvestre, C. M. Silva, Supercritical fluid extraction of vegetable matrices: Applications, trends and future perspectives of a convincing green technology, *J Supercrit Fluids*, **92**, 115-176 (2014).

[17]. F. Chemat, M. A. Vian, A. S. F. Tixier, M. Nutrizio, A. R. Jambrak, P. E. S. Munekata, J. M. Lorenzo, F. J. Barba, A. Binello, G. Cravotto, A review of sustainable and intensified techniques for extraction of food and natural products, Green Chemistry, **22**, 8, 2325-2353 (2020).

[18]. M. Herrero, J. A. Mendiola, A. Cifuentes, E. Ibáñez, Supercritical fluid extraction: Recent advances and applications, *J. Chromatogr. A*, **1217,** 16, 2495-2511 (2010).

[19]. N. Rombaut, Anne-Sylvie Tixier, A. Bily, F. Chemat, Green extraction processes of natural products as tools for biorefinery, *Biofuel. Bioprod. Biorefin*., **8**, 4, 530-544 (2014).

[20]. M. Perrut, Supercritical Fluid Applications: Industrial Developments and Economic Issues, *Ind. Eng. Chem. Res.,* **39**, 12, 4531–4535 (2000).

[21]. A. Saxena, B. P. Tripathi, M. Kumar, V. K. Shahi, Membrane-based techniques for the separation and purification of proteins: An overview, *Adv. Colloid Interface Sci.*, **145,** 1-22 (2009).

[22]. J. Ke, K. Yang, X. Bai, H. Luo, Y. Ji, J. Chen, A novel chiral polyester composite membrane: Preparation, enantioseparation of chiral drugs and molecular modeling evaluation, *Sep. Purif. Technol.,* **255**, 15, 117717 (2021).

[23]. M. C. Bubaloa, K. Radoševića, I. R. Redovnikovića, J. Halambekb,V. G. Srček, A brief overview of the potential environmental hazardsof ionic liquids, Ecotoxicol. Environ. Saf., **99**, 2-12 (2014).

[24]. R. Lemich, Adsoptive bubble separation methods-foam fractionation and allied techniques, *Ind., Eng., Chem*., **60**, 16-29 (1968).

[25]. C. Jiang, Z. Wu, R. Li, Q. Liu, Technology of protein separation from whey wastewater by two-stage foam separation, *Biochem. Eng. J.*, **55**, 43-48 (2011).

[26]. T. Kinoshitaa, Y. Ishigaki, N. Shibataa, K. Yamaguchi, S. Akita, S. Kitagawa, H. Kondou, S. Nii, Selective recovery of gallium with continuous counter-current foam Separation and its application to leaching solution of zinc refinery residues, *Sep. Purif. Technol.,* **78**, 181-188 (2011).

[27]. K. Kodama, M. Oiwa, T. Saitoh, Purification of rhodamine B by alcohol-modified air bubble flotation, *Bull. Chem. Soc. Jpn*., **94**, 1210-1214 (2021).

[28]. T. Saitoh, K. Shibata, K. Fujimori, Y. Ohtani, Rapid removal of tetracycline antibiotics from water by coagulation-flotation of sodium dodecyl sulfate and poly (allylamine hydrochloride) in the presence of Al (III) ions, *Sep. Purif. Technol.,* **187**, 31, 76-83 (2017).

[29]. J. Rubio, M. L. Souza, R.W. Smith, Overview of flotation as a wastewater treatment technique, *Miner. Eng.*, **15**, 3, 139-155 (2002).

[30]. Y. J. Liu, S. L. Lo, Y. H. Liou, C. Y. Hu, Removal of nonsteroidal anti-inflammatory drugs (NSAIDs) by electrocoagulation–flotation with a cationic surfactant, *Sep. Purif. Technol.,* **152**, 148-154 (2015).

[31]. P.Y. Bi, H. Ru. Dong, J. Dong, The recent progress of solvent sublation, *J. Chromatogr. A*, **1217,** 16, 2716-2725 (2010).

[32]. P. Y. Bi, D. Q. Li, H. R. Dong, A novel technique for the separation and concentration of penicillin G from fermentation broth: Aqueous two-phase flotation, *Sep. Purif. Technol.*, **69**, 2, 205-209 (2009).

[33]. L. Jakob, M. Heinzmann, H. Nirschl, Development of a continuous aqueous two-phase flotation process for the downstream processing of biotechnological products, *Sep. Purif. Technol.*, **278**, 1, 119657 (2021).

CHAPTER 2.

Evaluation of Solvent Property of Air-Water Interface Based on the Fluorescence Spectra of 1,2'-dinaphthylamine in the Aqueous Solution of Ultrafine Bubbles

2.1 Introduction

Adsorption of surfactants and amphiphilic substances to air-water interface has been well-known phenomenon [1-4]. These molecules orient hydrophilic group toward water while hydrophobic group toward air at the air-water interface. Molecular dynamics simulation studies have revealed the orientation of hydrophobic ions near the water surface [2]. Similarity between air-water interface and water-oil interface has been reported in molecular orientation [3]. These results suggest that air-water interface is more hydrophobic than bulk water. Polarity of air-water interface had been evaluated by the measurement of second harmonic spectra of polarity indicator molecules such as *N*,*N*-diethyl-4-nitroaniline and 4-(2,4,6-triphenylpyridinium)-2,6-diphenylphenoxide ($E_T(30)$) [5,6]. The results indicated that air-water interface has similar polarity to very nonpolar solvents such as *n*-heptane, carbon tetrachloride, and butyl ether. More recently, the property of air-water interface was found to be dependent on the structure of indicator molecule [7]. These studies have deepened our understanding of the property of the air-water interface. However, the second harmonic spectrometry requires expensive instruments and highly skilled experimental manipulations. Moreover, the spectra may be dependent on the orientation of indicator molecules at the air-water interface.

Recently, we have developed novel separation methods including non-surfactant air bubble flotation [8,9] and air bubble-assisted microfiltration [10]. In these methods, air bubbles act as a kind of adsorbent for basic dyes and drugs for their rapid and selective

separation in flotation or microfiltration techniques. Hydrophobicity was certainly an important factor for the adsorption onto air bubbles, but the results indicated the strong adsorption of rather polar or charged dyes and drugs. In the present study, fluorescent molecules that are responsive to solvent polarity as well as to ultrafine bubble concentration in water were explored. Three naphthylamine derivatives were tested as fluorescent probes. The air-water interface was supplied by generating ultrafine bubbles (UFB) for measuring emission spectra of fluorescent probes in homogeneous and clear aqueous solution. The UFB are defined as small air bubbles with a diameter less than 1 μm [11,12], and hence the solution was not turbid and found to be compatible with fluorescence spectroscopy in preliminary study. A naphthylamine derivative whose emission spectrum was the most sensitive to the presence of UFB was selected and compared with the spectra in different solvents to evaluate polarity or solvent property of air-water interface.

2.2 Expelimental

2.2.1 Chemicals

Fluorescent probes; *N*-phenyl-1-naphthylamine (PN), *N*-(4-biphenylyl)-1-naphthylamine (BPN), and 1,2'-dinaphthylamine (DN), were obtained from Tokyo Chemical Industry (Tokyo, Japan) and recrystallized three-time in aqueous ethanol. They were stored in a freezer (−20°C) as 1.0 mM ethanol solutions for PN and DN, and 0.25 mM ethanol solution for BPN. Water was purified with a Milli-Q Gradient Water Purification System (Merck Millipore, Burlington, MA, USA).

2.2.2 Generation of UFB

Water containing ultrafine bubbles (UFB solution) were prepared with an IDEC FZ1N-05D Ultrafine Bubble Generator (Osaka, Japan) utilizing the pressurized dissolution mechanism. It was 3 hours driving followed by 3 hours of rest, repeated 4 times. The dissolution pressure of air was 0.26 ± 0.01 MPa. Air used was passed through a non-woven filter to eliminate particulate materials. The concentration and size distribution of UFB were measured with a NanoSight LM10 nanoparticle tracking analysis instrument (Malvern Panalytical, Worcestershire, UK).

2.2.3 Fluorescence Analysis

The sample solution was prepared by adding 10 μL of fluorescent probe solution to 10 mL of water or UFB solution in a 15-mL glass tube while gently mixing with a vortex mixer. The fluorescence spectra were measured by using a JASCO FP-8300 Spectrofluorometer (Hachioji, JAPAN) with a 1-cm quartz cell. The emission wavelengths were 340 nm for PN, BPN, and DN. Slit widths of the excitation and mission wavelength were 5 nm.

2.3 Results and Discussion

Fig.2-1 shows concentration and size distribution of generated UFB. In the present experimental conditions, the UFB concentration was 1.09×10^9 pcs/mL. The concentration of UFB in diluted aqueous solution was proportional to the reciprocal of the dilution ratio with water. These results are consistent with reports of UFB concentration upon dilution of UFB solution with water [11-13]. From the result of Fig.2-1, the average size of UFB was 103 nm with 38 nm of the standard deviation. Compared to the high reproducibility in the result of the UFB concentration measurement, that of UFB size distribution measurement was less reproducible even in repeated measurements of the same sample.

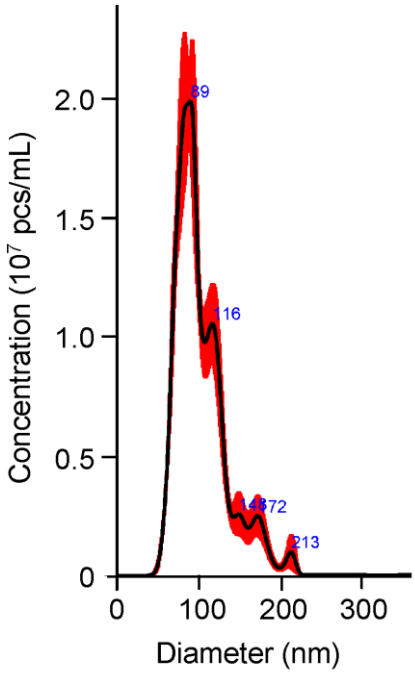

Fig.2-1 Size distribution of UFB in generated UFB water. The red area indicates the scatter of 5 measurements.

Fig. 2-2 shows emission spectra of PN, BPN, and DN in water and UFB solution. PN had been extensively used as a lipophilic probe for biomolecules [14-16] and an indicator for determining critical micelle concentrations of surfactants [17], because its emission strength enhanced and the spectrum shifted to lower wavelength due to the partitioning of the probe to the more hydrophobic region of the surfactant micelle. Such function of PN has been successfully utilized for evaluating hydrophobicity of microscopic environments of micelles or surfactant aggregates on solid surfaces [18,19] and surfactant-modified clay minerals (namely organoclays) [20]. However, the emission spectrum of PN changed negligibly in the presence of UFB. In our previous study, some degree of hydrophobicity was necessary for the adsorption onto air bubbles [9-11]. PN seems to have insufficient hydrophobicity for the effective adsorption on UFB. In contrast, the emission spectra of BPN and DN were remarkably changed by the presence of UFB, probably because they have enough hydrophobicity to adsorb onto the hydrophobic surfaces of the UFB and/or they adsorb more hydrophobic region on the surface of UFB. Due to the low solubility of BPN, however, it was difficult to obtain the clear emission spectrum. Moreover, there were low spectral change by the presence of UFB (Fig.2-2(B)). On the other hand, DN provided clear emission spectral change depending on the concentration of UFB (Fig.2-2(C)). The wavelength of the maximum emission (λ_{max}) of DN in water was 486 nm, while it shifted to shorter wavelength (408 nm) in the presence of ultrafine bubbles with a number concentration of 1.09×10^9 pcs/mL. This fact indicates that DN strongly partitions to the surface of the UFB which provided a much more nonpolar or hydrophobic microenvironment for DN relative to that it experiences in bulk water.

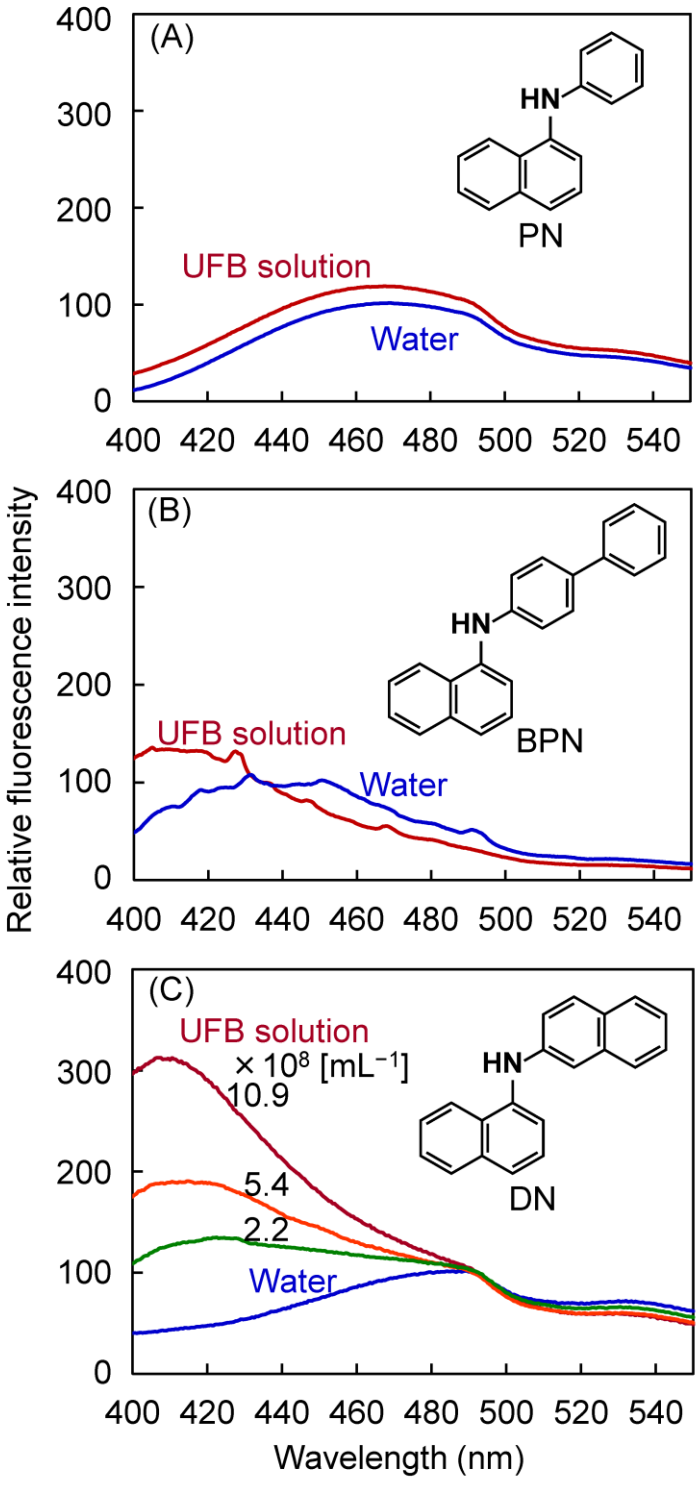

Fig.2-2 Emission spectra of PN (A), BPN (B), and DN (C) in water and UFB solution. Relative fluorescence intensity (100) was defined by the maximum emission intensity in water.

To briefly explain the concentration dependence observed for probe DN in the UFB. As seen in Fig.2-2(C), the emission wavelength of DN progressively shifts toward smaller values as the UFB concentration increases. This probably reflects the fact that a greater proportion of the DN partitions to and binds the more hydrophobic microenvironment of the UFB as the UFB concentration increases. That is, the equilibrium is shifted so that more DN in the bulk aqueous phase becomes bound to the UFB interface and thus at the greatest UFB concentration, is most likely completely bound:

$$\text{DN (aq)} + \text{UFB} \rightleftarrows \text{DN-UFB} \quad \text{(DN bound to interfacial region of UFB)}$$

The results obtained in the present study include adsorption isotherm of DN to the surface of the UFB. Accurate and reproducible measurements of the size distribution of the UFB, being essential for the accurate estimation of the surface area or interfacial region of the UFB, will enable quantitative analysis of adsorption isotherms.

Fig.2-3 shows the correlation of relative permittivity and λ_{max} value of DN in different solvents. The λ_{max} value in UFB solution indicating by an arrow was close to the values in ethyl acetate (416 nm) and diethyl ether (406 nm). The result strongly suggests that air-water interface has similar solvent property to ethyl acetate or diethyl ether that are extensively utilized as extracting solvents for a wide range of solutes including hydrophobic and rather polar organic compounds.

The property of the surface of UFB as an extracting solvent evaluated in the present study corresponded to that of ethyl acetate or diethyl ether. It was more hydrophilic rather than *n*-heptane, carbon tetrachloride, or butyl ether, clarifying by the measurement of second harmonic spectrometry using $E_T(30)$ [6,7]. The difference may be ascribable to the difference in the characteristics of indicator molecule or the difference in distance from air-water interface obtained by measurement method. According to the studies about the

orientation of organic and inorganic ions at the air-water interface [21-23], it can be inferred that the air-water interface has a polar or hygroscopic property that allows the distribution of these ions. The present result is consistent with the results obtained using more polar indicator molecules [8]. The result obtained in the present study would be useful when considering the properties of air-water interface as a selective collection medium for target substances.

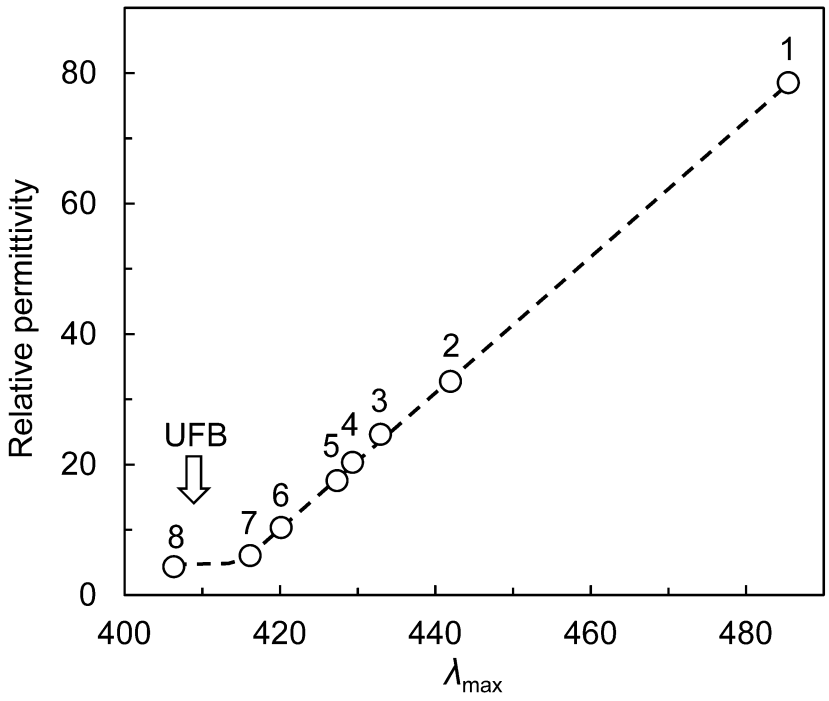

Fig.2-3 Correlation between relative permittivity of solvent and the wavelength at the maximum emission (λmax) of DN. Solvent: (1) water, (2) methanol, (3) ethanol, (4) 1-propanol, (5) 1-butanol, (6) 1-octanol, (7) ethyl acetate, (8) diethyl ether. An arrow indicates λmax value in water containing 1.09×10^9 [pcs/mL] of UFB.

2.4 Conclusion of This Chapter

It can be emphasized that this study is the first report to reveal the chemical properties of the surface or air-water interface of UFBs. Numerous studies about the stability and physical properties of UFBs have expanded the basics and application possibilities of the UFBs [24-28]. Differences in stability and physical properties from micro-bubbles as well as their size dependence are also interesting features of the UFBs. On the other hand, the chemistry or solvent property of UFBs or their surface has not received much attention. Development of a method to clarify the properties of ultrafine bubbles as a solvent, that is, their chemical properties, will facilitate the use of UFBs as separation media or reaction sites.

2.5 References

[1]. H. Mohwald, Phospholipid and phospholipid-protein monolayers at the air/water interface, *Annu. Rev. Phys. Chem*., **41**, 441-476 (1990). https://doi.org/10.1146/annurev.pc.41.100190.002301

[2]. H. M. McConnell, Structures and transitions in lipid monolayers at the air-water interface, *Annu. Rev. Phys. Chem*., **42**, 171-195 (1991). https://doi.org/10.1146/annurev.pc.42.100191.001131

[3]. C. H. Chang, E. I. Franses, Adsorption dynamics of surfactants at the air/water interface: a critical review of mathematical models, data, and mechanisms, *Colloid Surf. A Physicochem. Eng. Aspects,* **100**, 1-45 (1995). https://doi.org/10.1016/0927-7757(94)03061-4

[4]. J. Eastoe, J. S. Dalton, Dynamic surface tension and adsorption mechanisms of surfactants at the air-water interface, *Adv. Colloid Interface Sci*., **85**, 103-144 (2000). https://doi.org/10.1016/S0001-8686(99)00017-2

[5]. H. Wang, E. Borguet, K. B. Eisenthal, Polarity of liquid interfaces by second harmonic generation spectroscopy, *J. Phys. Chem. A,* **101**, 713-718 (1997). https://doi.org/10.1021/jp9806563

[6]. H. Wang, E. Borguet, K. B. Eisenthal, Generalized interface polarity scale based on second harmonic spectroscopy, *J. Phys. Chem. B,* **102**, 4927-4932 (1998). https://doi.org/10.1021/jp9806563

[7]. S. Sen, S. Yamaguchi, T. Tahara, Different molecules experience different polarities at the air/water interface, *Angew. Chem. Int. Ed*., **48**, 6439-6442 (2009). https://doi.org/10.1002/anie.200901094

[8]. K. Kodama, M. Oiwa, T. Saitoh, Purification of rhodamine B by alcohol-modified air bubble flotation, *Bull. Chem. Soc. Jpn*., **94**, 1210-1214 (2021). https://doi.org/10.1246/bcsj.20200395

[9]. K. Kodama, T. Saitoh, Surfactant-free air bubble flotation–coagulation for the rapid purifcation of chloroquine, *Anal. Sci*., **39**, 43-49 (2022). https://doi.org/10.1007/s44211-022-00196-2

[10]. K. Kodama, N. T. T. Thao, T. Saitoh, Effect of air bubbles on the membrane filtration of rhodamine B, *Anal. Sci.*, **39,** 1601-1605 (2023). https://doi.org/10.1007/s44211-023-00366-w

[11]. K. Terasaka, K. Yasui, W. Kanematsu, N. Aya, Ultrafine bubbles, Jenny Stanford Publishing, New York, USA, 2021. https://doi.org/10.1201/9781003141952

[12]. S. Tanaka, Y. Naruse, K. Terasaka, S. Fujioka, Concentration and dilution of ultrafine bubbles in water, *Colloids Interfaces 4*, **50** (2020). https://doi.org/10.3390/colloids4040050

[13]. D. Nieva-Gomez, J. Konisky, R. B. Gennis, Membrane changes in *Escherichia coli* induced by colicin Ia and agents known to disrupt energy transduction, *Biochemistry,* **15**, 2747-2753 (1976). https://doi.org/10.1021/bi00658a006

[14]. S. Ozeki, K. Tejima, Drug Interactions. V. Binding of basic compounds to bovine serum albumin by fluorescent probe technique, *Chem. Pharm. Bull*., **27**, 638-646 (1979). https://doi. org/10.1248/cpb.27.638

[15]. E. G. Sedgwick, P. D. Bragg, Distinct phases of the fluorescence response of the lipophilic probe *N*-phenyl-1-naphthylamine in intact cells and membrane vesicles of *Escherichia coli*, *Biochim. Biophys. Acta,* **894**, 499-506 (1987). https://doi.org/10.1016/0005-2728(87)90129-0

[16]. R. M. M. Brito, W. L. C. Vaz, Determination of the critical micelle concentration of surfactants using the fluorescent probe *N*-phenyl-1-naphthylamine, *Anal. Biochem.,* **152**, 250-255 (1986). https://doi.org/10.1016/0003-2697(86)90406-9

[17]. T. Saitoh, K. Taguchi, M. Hiraide, Evaluation of hydrophobic properties of sodium dodecylsulfate/γ-alumina admicelles based on fluorescence spectra of *N*-phenyl-1-naphthylamine, *Anal. Chim. Acta*, **454**, 203-208 (2002). https://doi.org/10.1016/S0003-2670(01)01575-6

[18]. T. Saitoh, K Shibata, M Hiraide, Rapid removal and photodegradation of tetracycline in water by surfactant-assisted coagulation-sedimentation method, *J. Environ. Chem1016. Eng.,* **2**, 1852-1858 (2014). https://doi.org/10. /j.jece.2014.08.005

[19]. T. Saitoh, T. Shibayama, Removal and degradation of β-lactam antibiotics in water using didodecyldimethylammonium bromide-modified montmorillonite organoclay, *J. Hazard, Mater.,* **317**, 677-685 (2016). https://doi.org/10.1016/j.jhazmat.2016.06.003

[20]. P. Jungwirth, D. J. Tobias, Ions at the air/water interface, *J. Phys. Chem. B*, **106**, 6361-6373 (2002). https://doi.org/10.1021/jp020242g

[21]. P. Jungwirth, D. J. Tobias, Specific ion effects at the air/water interface, *Chem. Rev.*, **106**, 1259-1281 (2006). https://doi.org/10.1021/cr0403741

[22]. Y. Rao, M. Subir, E. A. McArthur, N. J. Turro, K. B. Eisenthal, Organic ions at the air/water interface, *Chem. Phys. Lett.,* **477**, 241-244 (2009). https://doi.org/10.1016/j.cplett.2009.07.011

[23]. F. Y. Ushikubo, T. Furukawa,. Nakagawa, M. Enari, Y. Makino, Y. Kawagoe, T. Shiina, S. Oshita, Evidence of the existence and the stability of nano-bubbles in water, *Colloids Surf. A Physicochem*., **361**, 31-37 (2010). https://doi.org/10.1016/j.colsurfa.2010.03.005

[24]. W. Kanematsu, T. Tuziuti, K. Yasui, The influence of storage conditions and container materials on the long term stability of bulk nanobubbles - Consideration from a perspective of interactions between bubbles and surroundings, *Chem. Eng. Sci*., **219**, 115594 (2020). https://doi.org/10.1016/j.ces.2020.115594

[25]. X. Zhang, Q. Wang, Z. Wu, D. Tao, An experimental study on size distribution and zeta potential of bulk cavitation nanobubbles, *Int. J. Min. Met. Mater.,* **27**, 152-161 (2020). https://doi.org/10.1007/s12613-019-1936-0

[26]. S. Tanaka, K. Terasaka, S Fujioka, Generation and long-term stability of ultrafine bubbles in water, *Chem. Ing. Tech. (Weinh)*, **93**, 168-179 (2021). https://doi.org/10.1002/cite.202000143

[27]. B. H. Tan, H. An, C.-D. Oh, Stability of surface and bulk nanobubbles, *Curr. Opin. Colloid Interface Sci.,* **53**, 101428 (2021). https://doi.org/10.1016/j.cocis.2021.101428

CHAPTER 3.

Surfactant-free Air Bubble Flotation–Coagulation for the Rapid Purification of Chloroquine

3.1 Introduction

Chloroquine (CQ) is a popular medicine that has long been used as an antimalaria medication [1]. According to the 2020 World Malaria Report of WHO, the disease onset patient was 229 million people with 409,000 deaths in 2019 [2]. Malaria is still a serious disease threat which has not declined yet. Despite of the occurrence of CQ-resistant malaria, CQ and its analogues have been antimalarial of choice for several decades because of the effectiveness, large tolerance, safety, and relatively low price. Moreover, CQ derivatives have recently been studied as effective therapeutic drug candidates for different viral infections, cancer, immune, neoplastic, and neurological diseases [3-8]. These facts indicate that CQ remains a solid candidate for the treatment of various diseases.

CQ is typically synthesized by an S_N2 reaction of 4,7-dichloroquinoline and 4-amino-1-diethylaminopentane (Fig.3-1) [9,10]. The crude product is extracted into an appropriate organic solvent and then recrystallized to obtain high purity CQ. Considerable amounts of toxic, volatile, and flammable organic solvents are used to perform these purification processes. Moreover, energy consumption for temperature control and time-

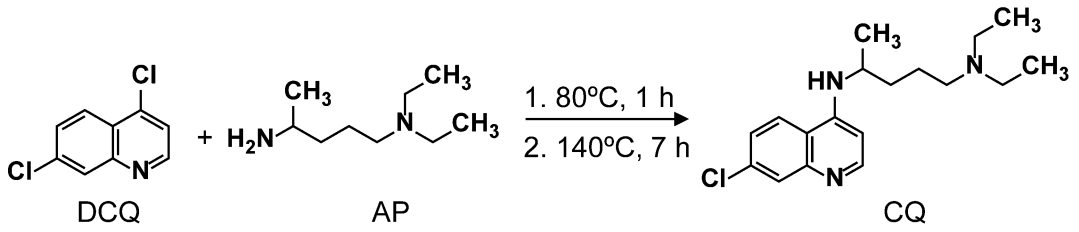

Fig.3-1 Reaction scheme of CQ

consuming procedures are necessary in the respective purification steps.

Recently, we have designed a novel separation method for the purification of a fluorescent dye, Rhodamine B, from its crude product [11]. The method was conducted by placing an aqueous solution containing crude Rhodamine B in a cylindrical flotation vessel having a sintered glass filter followed by feeding air through the filter to generate air bubbles. In the presence of small amount (0.2~0.5% (v/v)) of ethanol, Rhodamine B was enriched to temporary generated foam on the surface of water, while reactants and intermediate compounds remained in the bulk aqueous solution. By three-times repeated separation, reactants, intermediate compounds reduced into undetectable levels. The method was applicable to obtain high-purify (>99.8%) Rhodamine B.

Because of very simple and rapid procedures as well as needless of large amount of toxic and flammable organic solvents, air bubble flotation may become a useful basis as a drug purification method. Different from conventional surfactant-mediated flotation techniques, purified product does not contain surfactants or collector molecules that are difficult to separate. In the present study, we examined the applicability of air bubble flotation for CQ purification. Experimental conditions required for the selective CQ separation were investigated in detail. Physicochemical and computational chemical approaches were applied to clarify the mechanism of the adsorption and coagulation of CQ at air-water interface. Repeated air bubble flotation was tested for obtaining high-purity CQ from its crude product.

3.2 Experimental

3.2.1 Chemicals

Chloroquine (CQ) diphosphate (>98.0%), 4,7-dichloroquinoline (DCQ), and 4-amino-1 diethylaminopentane (AP) were obtained from Tokyo Chemical Industry (Tokyo, Japan). 2-Propanol and sodium hydroxide (for medicine test) were purchased from Fujifilm Wako Pure Chemical (Osaka, Japan). Other reagents used was of analytical grade. Water was prepared with a Milli-Q Integral Water Purification System (Merck Millipore, Billerica, MA, USA). Crude CQ was obtained by a minor modification of the synthetic method reported by F.A.R. Ruiz, *et al*. [10]. A 500-mg portion of DCQ and 2.00 g of AP were placed in a 50 mL round bottom flask. The mixture was heated at 80 ℃ for 1h and then, the temperature was raised to 140 ℃ to continue the reflux for 7h. It was dissolved in 2 mL of 2-propanol and then volumetrically up to 10 mL with water to prepare a crude CQ solution.

3.2.2 Flotation of CQ

A cylindrical open glass column (length: 700 mm, inner diameter: 50 mm, for column chromatography, GL Science, Tokyo, Japan) with a sintered glass filter (pore size: 20~30 μm) at the bottom was used as a flotation vessel. The pore size of the glass filter was selected because of the smooth air feeding to generate sufficient amount of air bubbles. One milliliter each of crude CQ solution and 10 M NaOH were poured into 1 L of water. The resulting solution (pH 12) was placed in the flotation vessel and then air (0.4 L min^{-1}) was supplied through the sintered glass filter to generate air bubbles. After conducting air bubble flotation for 90 seconds, coagulates formed on the surface of water was collected with a suction. The coagulates were washed with cold water and then dissolved with 2 mL of 2-propanol to pour into another flotation vessel in which 1.0 L of 0.01 M sodium hydroxide solution was placed. The air bubble flotation was repeated 3

times. Finally, the coagulates were washed with cold water on an Omnipore™ membrane filter (hydrophilic PTFE, pore size: 0.45 μm, Merck Millipore) and then dissolved with 10 mL of 2-propanol. Bulk aqueous solution was also sampled from the bottom of the flotation vessel to monitor the residual concentrations of the respective compounds.

A Waters LC-MS system (Milford, MA, USA) composing of an Alliance e2695 separations module, a 2439 UV/Vis spectrophotometric detector, and a 3100-type mass spectrometric detector with connecting an InertSustain™ C18 column (length: 150 mm, inner diameter: 3.0 mm, particle size: 3.0 μm, GL Science, Tokyo, Japan) for the separation and determination of CQ and DCQ. The mobile phase composition was initially 40% (v/v) acetonitrile containing 5 mM triethylamine and 10 mM ammonium acetate for 7 min and, then, followed by elevating acetonitrile content to 80% (v/v) continued for 6 min. The flow rate and detection wavelength were 0.5 mL min^{-1} and 250 nm, respectively. Ionization potential (positive ion mode) and souse temperature of mass spectrometric detector were 20 V and 120°C. A Shimadzu GC-2014 gas chromatographic system having an FID detector (Kyoto, Japan) was used for the separation and determination of CQ and AP. A capillary column employed was TC-WAX (GL Science, liquid phase: polyethylene glycol, inner diameter: 0.25 mm, length: 30 mm). Linear flow velocity of carrier gas, N2, was 23 cm s^{-1}. Column oven temperature was initially 85°C for 3 min, then ramped by 50°C min^{-1}, held at 190°C for 4 min, ramped by 30°C min^{-1}, and finally held at 230°C for 6 min.

3.2.3 Dynamic Surface Tension Measurement

Dynamic surface tension was measured with a potable dynamic tensiometer Dyno Tester^{+} (SITA Messtechnik, Dresden, Germany), in which air bubbles are generated in the solution, and the surface tension is measured from the pressure applied to the air bubbles. Before measurement, aqueous solutions containing 0.1% (v/v) of 2-propanol and prescribed amount of CQ or DCQ were placed in a water bath whose temperature (25.0 ± 0.2°C) was controlled with a CTP-1000 low temperature circulator (EYERA, Tokyo, Japan).

3.2.4 Solubility Measurement

For measuring the solubilities of CQ and DCQ, they were dissolved in 0.01 M sodium hydroxide containing 0.1% (v/v) of 2-propanol by mixing for 96 h at 25.0 ± 0.2°C. The solution was passed through an Omnipore^{TM} hydrophilic PTFE membrane filter (pore size: 0.2 μm) to eliminate insoluble fraction. A Jasco Extrema HPLC system (Hachioji, Japan) composing of a PU-8140 RHPLC pump and a UV-4075 Vis/UV detector was used for the determination of CQ and DCQ. The separation column, mobile phase composition, detection wavelength, and other chromatographic conditions were the same as those described above.

3.2.5 Molecular Dynamic Simulation

A Winmoster^{TM} (X-Ability, Tokyo, Japan) was used for driving a large-scale atomic/molecular massively parallel simulator (LAMMPS). An EliteDesk 800G5 desk-top personal computer (Win 10, 32 GB, HP Japan, Tokyo, Japan) was employed for calculating the simulation.

3.3 Results and Discussion

3.3.1 Air Bubble Flotation

About 60 seconds after the start flotation, occurrence of white coagulates was found at the top of the foam temporally generating on the surface of water. This phenomenon is ascribable to the enrichment of CQ beyond its saturation concentration around the surface of water. Time-dependent removal ratios of CQ and DCQ are shown in Fig.3-2, in which their initial concentrations are 10 μM. The removal ratio (%) was calculated by the following equation.

$$\text{Removed (\%)} = \frac{(C_0 - C)}{C_0} \times 100 \quad \cdot\cdot\cdot (1)$$

Here, C_0 denotes initial concentration and C is the concentration remaining in the bulk aqueous solution. The removal ratio of CQ reached maximum after 90 seconds and remained a constant value (95 ± 1%) while the value of DCP was only 20 ± 3%, indicating the achievement of selective separation of CQ.

Fig.3-3 shows the effect of pH on the removal ratio of CQ and DCQ. CQ was hardly separated at pH 7 while it was well enriched on the surface of water at pH 12. Such pH dependence of CQ separation can be ascribed to the pH dependent acid-base property of CQ. CQ (pK_a: 10.47 and 6.33 [12]) can protonate to form its positively charged conjugated acid in the neutral pH region, while it becomes uncharged species having higher hydrophobicity that can be represented by aqueous-octanol distribution coefficient (log K_{ow} = 4.63 [13]). The value is greater than that for DCQ (log K_{ow} = 3.57 [13]). Solute hydrophobicity was an important factor for the adsorption on the surface of air bubbles. Therefore, the solution pH was set to 12 for separating CQ from DCQ.

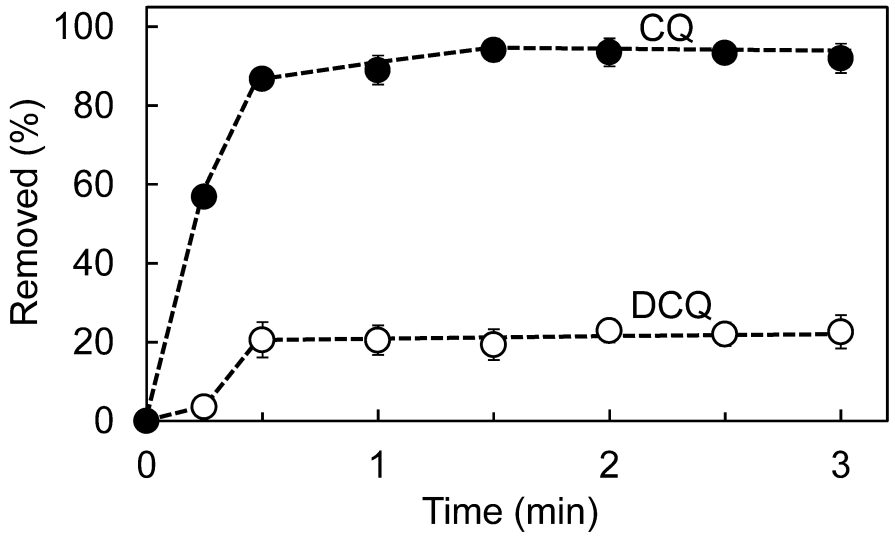

Fig.3-2 Effect of flotation time on the removal of CQ and DCQ

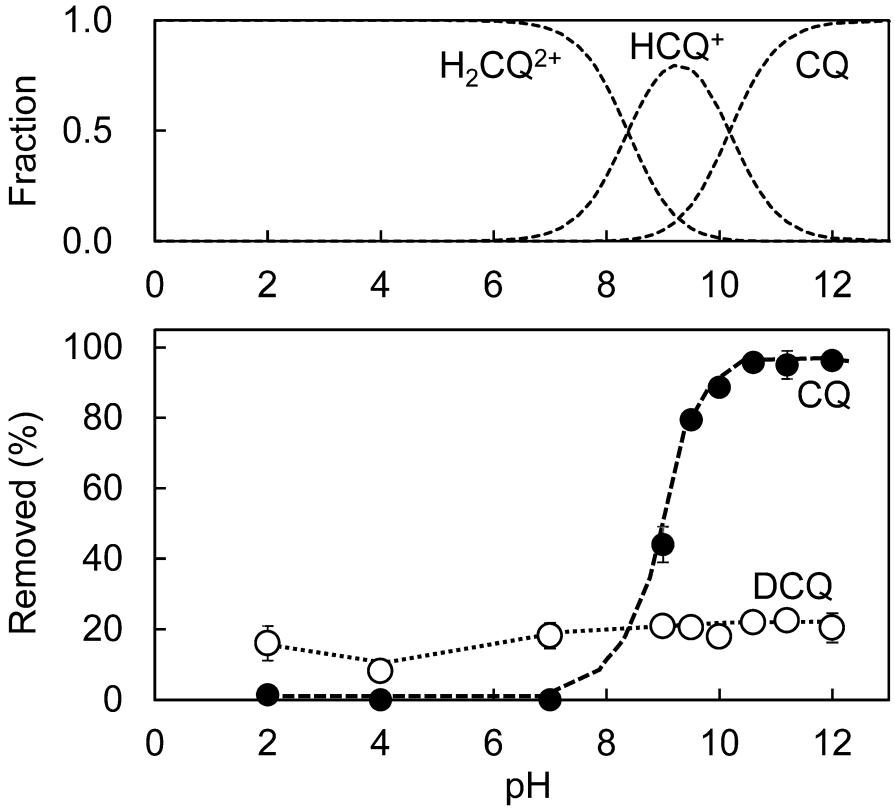

Fig.3-3 Effect of solution pH on the removal of CQ and DCQ. The fig ure above is pH-dependent mole fraction of CQ

The adsorption of CQ and DCQ onto the surface of air bubbles can be evaluated by measuring the dynamic surface tensions of their aqueous solutions. Fig.3-4 shows dynamic surface tension, γ [mN m^{-1}], of the aqueous solutions containing different amount of CQ or DCQ. At pH 12, the surface tension of DCQ solution was almost independent of the concentration of DCQ, indicating that DCQ hardly adsorbs on the air water interface. In contrast, that of CQ solution decreased with increasing the concentration of CQ because of its adsorption on the air-water interface. Arrows in Fig.3-4 indicate the solubilities of CQ (35.6 ± 0.4 μM) and DCQ (166 ± 6 μM) in the aqueous solution (pH 12) containing 0.1% (v/v) of 2-propanol. The decrease in the surface tension of CQ solution was more significant in the concentration range above the solubility of CQ, suggesting that CQ coagulates more strongly adsorb on the air-water interface rather than a CQ molecule. This fact was advantageous for the selective collection of CQ. At pH 7, the surface tension was almost independent of the concentration of CQ, supporting non-adsorptive property of positively charged conjugated acid of CQ.

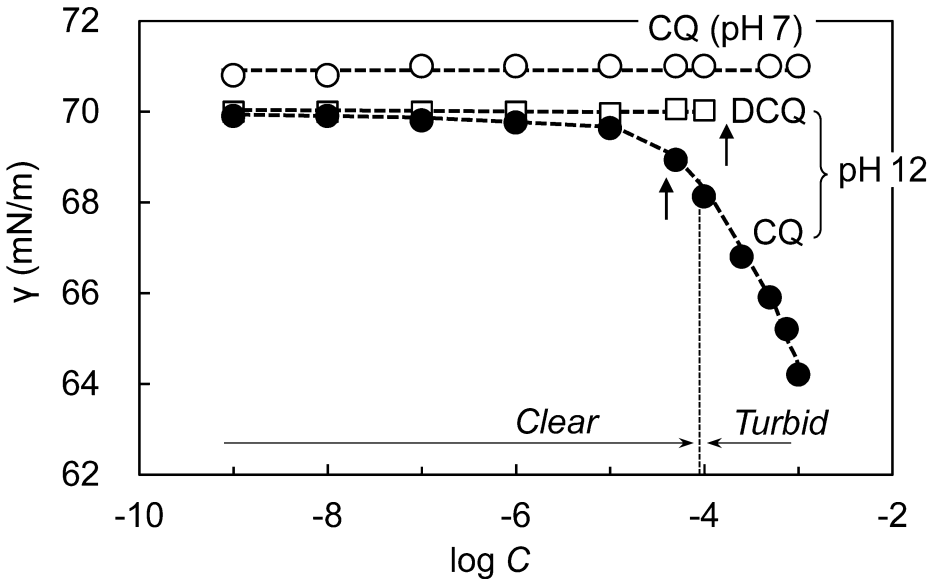

Fig.3-4 Dynamic surface tension of aqueous solution containing different amount of CQ or DCQ. Arrows indicate the solubilities of the respective compounds

The behavior of CQ close to the air-water interface may also be demonstrated by a molecular dynamic simulation method. Different simulation methods have been reported to reproduce the dynamics of ions or molecules at the air-water interface [14-16]. In the present study, LAMMPS was employed to visualize the dynamic behavior of CQ. The intermolecular force on a molecule is represented by the sum of the interaction on a molecule located at a position.

$$f_i = \sum_{I \neq i} f(r_{ij}) \quad \cdot \cdot \cdot (2)$$

The intermolecular force can also be expressed by the Newtonian equation of motion.

$$ma_i = m \frac{d^2 r_i}{dt^2} = f_i \quad \cdot \cdot \cdot (3)$$

Here, m [kg] denotes the mass of a molecule (or ion), a_i [m s^{-2}] is the acceleration of the molecule, r_i [m] is the position of the molecule, and t [s] is time. Fig.5 shows the results of the dynamic molecular simulation of one molecule of CQ (A) or 30 molecules of CQ (B) in water. As indicated in Fig.3-5(A), a CQ molecule placed at the random position in water moved to adsorb on the air-water interface. Moreover, multiplex of CQ molecules adsorbed on the air-water interface to form coagulate (Fig.3-5(B)). These results strongly support the experimental results including the enrichment and coagulation of CQ on the surface of water in the air bubble flotation.

Next, the effect of initial concentration was studied to clarify the sample loading capacity of the proposed method. Fig. 3-6 shows the effects of the initial concentrations of CQ and DCQ on their removal ratios. The values increased with increasing the initial concentrations because of the easy formation of the coagulates. However, selectivity in the removal of CQ decreased with increasing the initial DCQ concentration more than 10 μM (2 mg L^{-1}) due to the increased formation of DCQ precipitates.

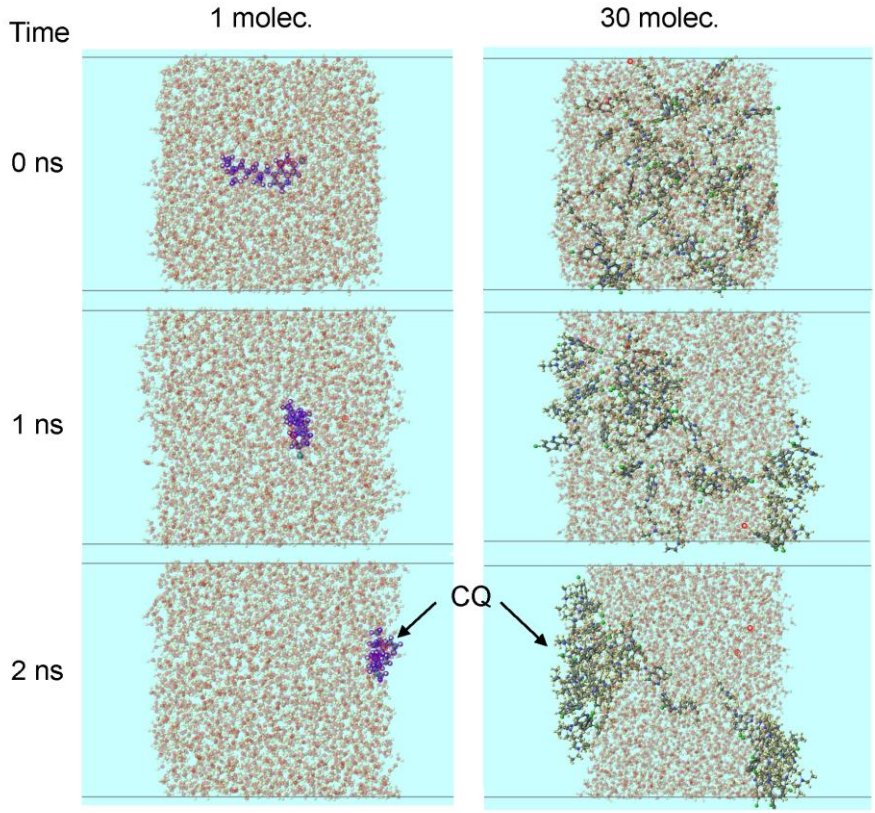

Fig.3-5 Results of molecular dynamic simulation (LAMMPS) of one or 30 molecules of CQ close to air–water interface

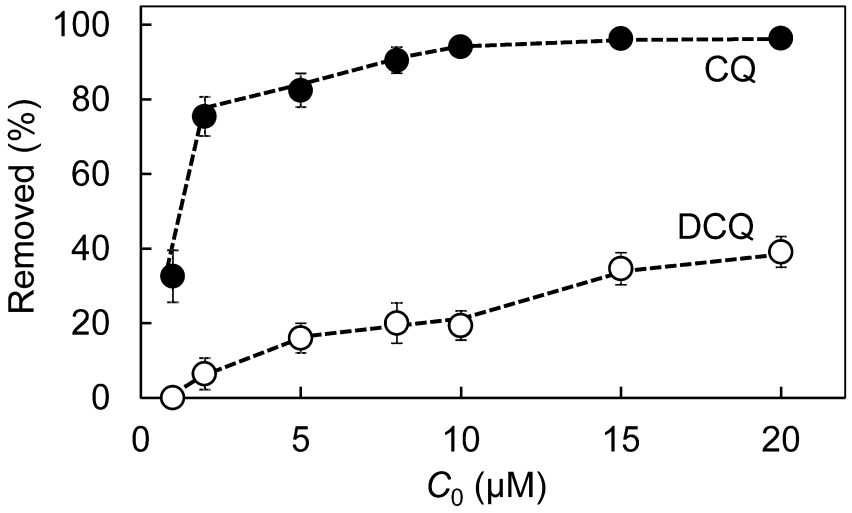

Fig.3-6 Effect of initial concentration, C_0, on the removal of CQ and DCQ

Before the application to CQ purification, the recoveries of 10 μM each of CQ and DCQ from the mixed solution were clarified. Fig. 3-7 shows the recoveries of CQ and DCQ obtained by conducting repeated air bubble flotation. Here, the recovery was defined by the ratio of the amount recovered (W_i) after the respective times of the flotation to the initial amount (W_0) in the crude product and taken into consideration of loss during suction collection.

$$\text{Recovery}\ (\%) = \frac{W_i}{W_0} \times 100 \quad \cdot \cdot \cdot (4)$$

The recovery of CQ was 72 ± 8% after three times separation, while the amount of DCQ reduced into undetectable level. As indicated in Fig. 3-6, removal ratio was dependent on the initial concentrations of CQ and DCQ. Since the amount of sample load was optimized for target CQ, the initial concentration of DCQ estimated was below 2 μM. Preferential adsorption of CQ onto air-water interface may be another reason for the low recovery of DCQ and, therefore, high selectivity for CQ. Estimated time for three times separation was within 15 min, being extremely shorter than the time required for recrystallization, sublimation, or chromatographic separation.

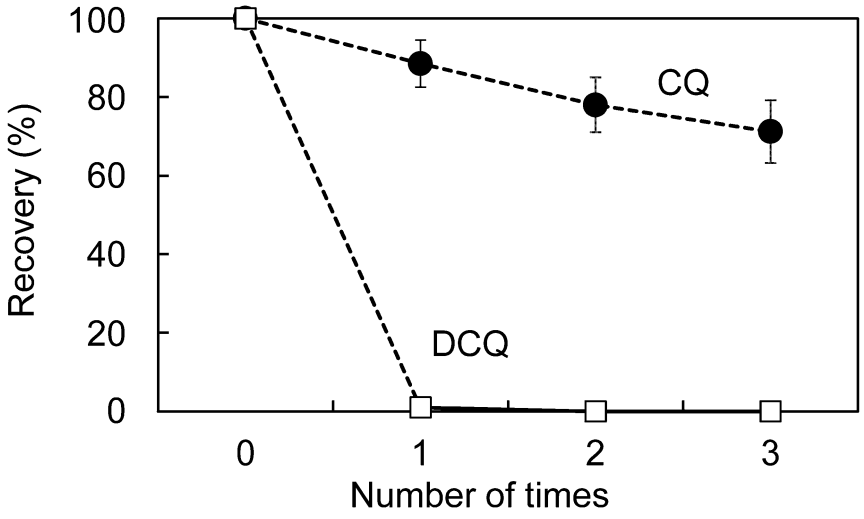

Fig.3-7 Recoveries of CQ and DCQ after the respective time of air bubble flotation

3.2.2 Application to CQ Purification

Fig. 3-8 shows liquid chromatograms obtained by introducing crude CQ solution (A), purified CQ solution obtained by conducting air bubble flotation three times (B), and a solution of standard material of CQ (C). It also indicates mass spectrum ($[CQ+H]^+$ = 320.3) for the peak (retention time = 6.4 min) in an enclosure. A peak of DCQ and some unknown peaks that appeared in the chromatogram of crude CQ (Fig.3-8(A)) reduced into undetectable levels in that of purified CQ (Fig.3-8(B)). The chromatogram of purified CQ was almost the same as that of standard material of CQ (Fig.3-8(C)). The existence of excess AP was monitored by GC as indicated in Fig. 9. Definite peaks of AP and DCQ as well as several unknown peaks observed in the gas chromatogram of crude CQ (Fig. 3-9(A)) also reduced into undetectable levels in the chromatogram of purified CQ (Fig.3-9(B)). The purity of CQ estimated based on the peak areas at detection wavelength 250 nm in liquid chromatogram was >99.0%. White granules of CQ was finally obtained by washing the coagulate with cold water and then freeze-drying it. The result obtained in the present study strongly suggests applicability of non-surfactant air bubble flotation for the rapid and simple purification of CQ. The studies about scaling-up and continuous processing may be important for the practical application to drug purification.

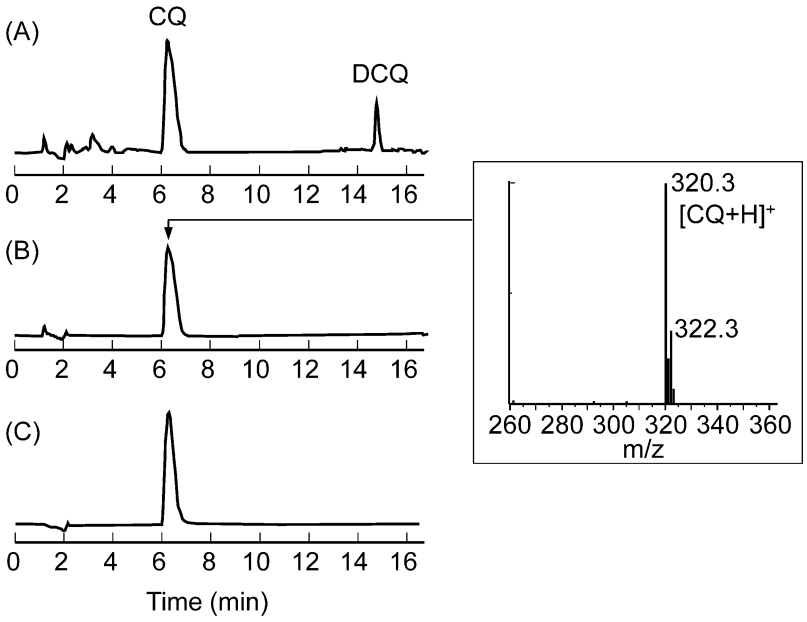

Fig. 3-8 Liquid chromatograms of crude CQ (a), purified CQ (b), and standard material of CQ (c) obtained by ultra-violet detection at 250 nm and ESI-mass spectrum obtained by introducing a fraction of CQ

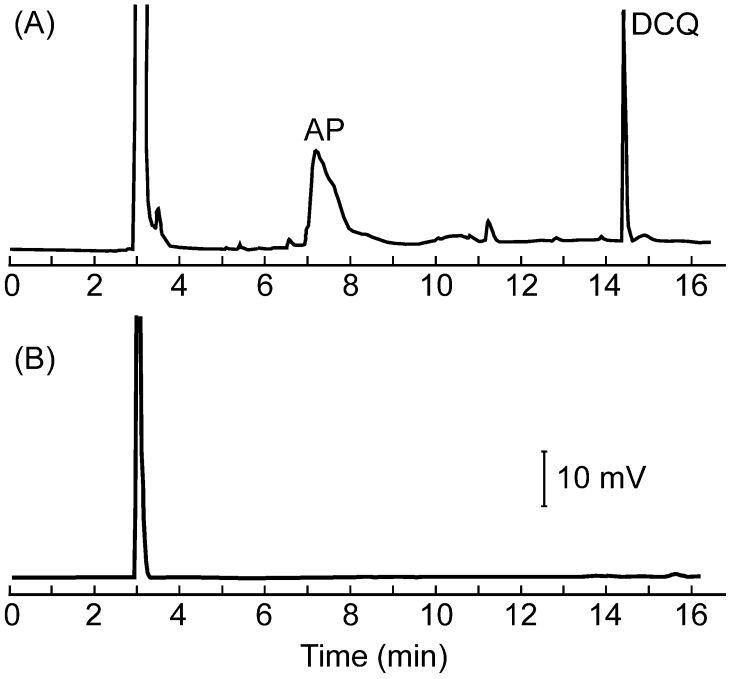

Fig. 3-9 Gas chromatograms obtained by introducing crude CQ (a) and purified CQ (b). A peak of CQ was not detectable in the experimental period because of its very low volatility.

3.4 Conclusion of This Chapter

Non-surfactant air bubble flotation was a rapid and simple separation method for the purification of chloroquine (CQ) from its crude product. CQ in the aqueous solution containing 0.1% (v/v) 2-propanol was enriched to form coagulate on the top of the foam temporary generated on the surface of water. The results of dynamic surface tension measurement and molecular dynamic simulation indicated selective adsorption and coagulation of CQ on the surface of air bubbles or air-water interface. At pH 12, CQ was selectively collected as the coagulates to the surface of water within 90 seconds, while other constituents including source materials and impurities remained in the bulk aqueous solution. High-purity (>99.0% as a 250 nm detection in HPLC) CQ was obtained by performing three times air bubble flotation.

3.5 References

[1]. R. Thomé, S.C.P. Lopes, F.T.M. Costa, L. Verinaud, L. Verinaud, Chloroquine: Modes of action of an undervalued drug, *Immunol. Lett*., **153** (2013) 50-57. https://doi.org/10.1016/j.imlet.2013.07.004

[2]. WHO. World malaria report 2020: 20 years of global progress and challenges. Geneva: World Health Organization; 2020. https://www.who.int/publications/i/item/9789240015791

[3]. A. Savarino, L.D. Trani, I. Donatelli, R. Cauda, A. Cassone, New insights into the antiviral effects of chloroquine, *Lancet. Infect. Dis*., **6** (2006) 67–69. https://doi.org/10.1016/S1473-3099(06)70361-9

[4]. P. Maycotte, S. Aryal, C.T. Cummings, J. Thorburn, Chloroquine sensitizes breast cancer cells to chemotherapy independent of autophagy, *Autophagy* **8** (2012) 200-211. https://doi.org/10.4161/auto.8.2.18554

[5]. M.A.A. Al-Bari, Targeting endosomal acidification by chloroquine analogs as a promising strategy for the treatment of emerging viral diseases, **5** (2017) e00293. https://doi.org/10.1002/prp2.293

[6]. Y. W. Tan, W. K. Yam, J. Sun, J. J. H. Chu, An evaluation of chloroquine as a broad-acting antiviral against hand, foot and mouth disease, *Antiviral Res*., **149** (2018) 143–149. https://doi.org/10.1016/j.antiviral.2017.11.017

[7]. D. Plantone, T. Koudriavtseva, Current and future use of chloroquine and hydroxychloroquine in infectious, immune, neoplastic, and neurological diseases: a mini-review, *Clin. Drug Investig*., **38** (2018) 653–671. https://doi.org/10.1007/s40261-018-0656-y

[8]. A. W. Zhou, H. Wang, Y. Yang, Z.S. Chen, C. Zou, Chloroquine against malaria, cancers and viraldiseases, *Drug Discovery Today,* **25** (2020) 2012–2022. https://doi.org/10.1016/j.drudis.2020.09.010

[9]. W.S. Johnson, B.G. Buell, A new synthesis of chloroquine, *J. Am. Chem. Soc.,* **74** (1952) 4513–4516. https://doi.org/10.1021/ja01138a014

[10]. F.A.R. Ruiz, R.N. García-Sánchez, S.V. Estupiñan, A. Gómez-Barrio, D.F.T. Amado, B.M. Pérez Solórzano, J.J. Nogal-Ruiz, A.R. Martínez-Fernández, V.V. Kouznetsov, Synthesis and antimalarial activity of new heterocyclic hybrids based on chloroquine and thiazolidinone scaffolds, *Bioorg. Med. Chem.,* **19** (2011) 4562–4563. https://doi.org/10.1016/j.bmc.2011.06.025

[11]. K. Kodama, M. Oiwa, T. Saitoh, Purification of Rhodamine B by alcohol-modified air bubble flotation, *Bull. Chem. Soc. Jpn*., **94** (2021) 1210–1214. https://doi.org/10.1246/bcsj.20200395

[12]. C. Rendal, K.O. Kusk, S. Trapp, The effect of pH on the uptake and toxicity of the bivalent weak base chloroquine tested on Salix viminalis and Daphnia magna, *Environ. Toxicol. Chem*., **30** (2011) 324–359. https://doi.org/10.1002/etc.391

[13]. A. Breindl, B. Beck, T. Clark, Prediction of the n-octanol/water partition coefficient, log P, Using a combination of semiempirical MO-calculations and a neural network, *J. Mol. Model*., **3** (1997) 142–155. https://doi.org/10.1007/s008940050027

[14]. M. Mucha, B. Minofar, P. Jungwirth, E.C. Brown, D.J. Tobias, Propensity of soft ions for the air/water interface, *Curr. Op. Colloid In*., **9** (2004) 67-73. https://doi.org/10.1016/j.cocis.2004.05.02

[15]. P. Jungwirth, D.J. Tobias, Specific ion effects at the air/water interface, *Chem. Rev*., **106** (2006) 1259 1281. https://doi.org/10.1021/cr0403741

[16]. Y.L.S. Tse, C. Chen, G.E. Lindberg, R. Kumar, G.A. Voth, Propensity of hydrated excess protons and hydroxide anions for the air-water interface, *J. Am. Chem. Soc*., **137** (2015) 12610–12616. https://doi.org/10.1021/jacs.5b07232

CHAPTER 4.

Effect of Air Bubbles on the Membrane Filtration of Rhodamine B

4.1 Introduction

Membrane filtration is a popular technique for separating particulate matters as well as even dissolved substances [1,2]. Particularly, nanofiltration membranes have extensively been used for the rejection of small molecules or organic ions in water [3,4]. In the practical use, these membranes are modularized and the water to be treated is pressurized and supplied to the module. However, the requirement of pressurization lead to larger equipment and higher operation costs. The reason of the necessity of the pressurization is ascribable to the extremely small pore size of the membranes. Recent development in the membrane technology enabled the development and application of gravity-driven membrane filtration using ultrafiltration membranes [5]. However, molecular size that can be separated by the ultrafiltration membrane is in the range of 20–100 kDa being far greater than the molecular weights of small organic molecules such as dyes, pharmaceuticals, and other analytes. Use of larger pore size membranes such as microfiltration membranes or membrane filters can reduce the pressure required and increase the throughput, but these filters do not have the ability to reject dissolved organic molecules and ions.

Recently, we reported a surfactant-free air bubble flotation for the purification of a basic dye, rhodamine B (RB) in water [6]. The method was conducted by feeding air bubbles from the bottom of a cylindrical vessel in which the aqueous solution containing crude RB had been placed. RB in the aqueous solution was rapidly enriched to the surface of water with separating source materials and intermediate compounds to obtain the highly purified product. In this system, air bubbles act as adsorbents for the selective collection of RB. The properties of air bubbles as an adsorbent may also be applied to

membrane separation. Since the sizes of air bubbles are larger than the pore size of the membrane filter present in the aqueous solution and a target substance is adsorbed to the air bubbles, it may be possible to prevent the passage of the target substance through the membrane filter.

In this section, we studied the feasibility of the use of air bubbles to achieve membrane filtration of a small organic molecule, RB. For this purpose, the aqueous solution containing RB was passed through a membrane filter with generating air bubbles by vigorous mixing of the solution using a homogenizer. The correlation of the amount of air bubbles and rejection efficiency of RB was investigated. Behavior of another dye, methylene blue (MB), was also observed to clarify the factor influencing the rejection efficiency.

4.2 Experimental

4.2.1 Chemicals

RB and MB (ion association agents for spectrophotometric analysis) were obtained from Tokyo Chemical Industry (Tokyo, Japan). 1-Butanol purchased from Fujifilm Wako Pure Chemical (Osaka, Japan) was used as a frother. Water was purified with a Milli-Q Gradient Water Purification System (Merk Millipore, Burlington, MA, USA). A homogenizer T18 digital Ultra-Turrax® (IKA, Staufen, Germany) with a shaft generator S18N-19G (shaft diameter: 19 mm, generator outer diameter: 19 mm, rotor diameter: 12 mm) was used for generating air bubbles. An Omnipore™ hydrophilic PTFE membrane filter (pore size: 0.20 μm, diameter: 45 mm, Merk Millipore) was employed for the membrane separation.

4.2.2 Filtration

The setting of a membrane filter on the filtration equipment and its outline including the immersed part of a shaft generator and illustrated in Fig.1 The membrane filter was placed on a filter base fitted with a stainless support screen and then a 300 mL glass funnel (inner diameter: 70 mm) was placed on it. The filtration equipment was set on a suction filtration bell in which a 100 mL beaker was placed for collecting filtrate solution. A 200-mL portion of the aqueous solution containing 0.05% (v/v) of 1-butanol and 5.0×10^{-6} mol dm^{-3} of RB or MB was placed in the glass funnel, the shaft generator of the homogenizer was immersed in the solution and then rotated at high speed to generate air bubbles. The rotation speed was in the range of 4,000–24,000 rpm. A 20-mL portion of aqueous solution passed through the membrane filter was collected to measure the absorbance at 556 nm for RB and 664 nm for MB.

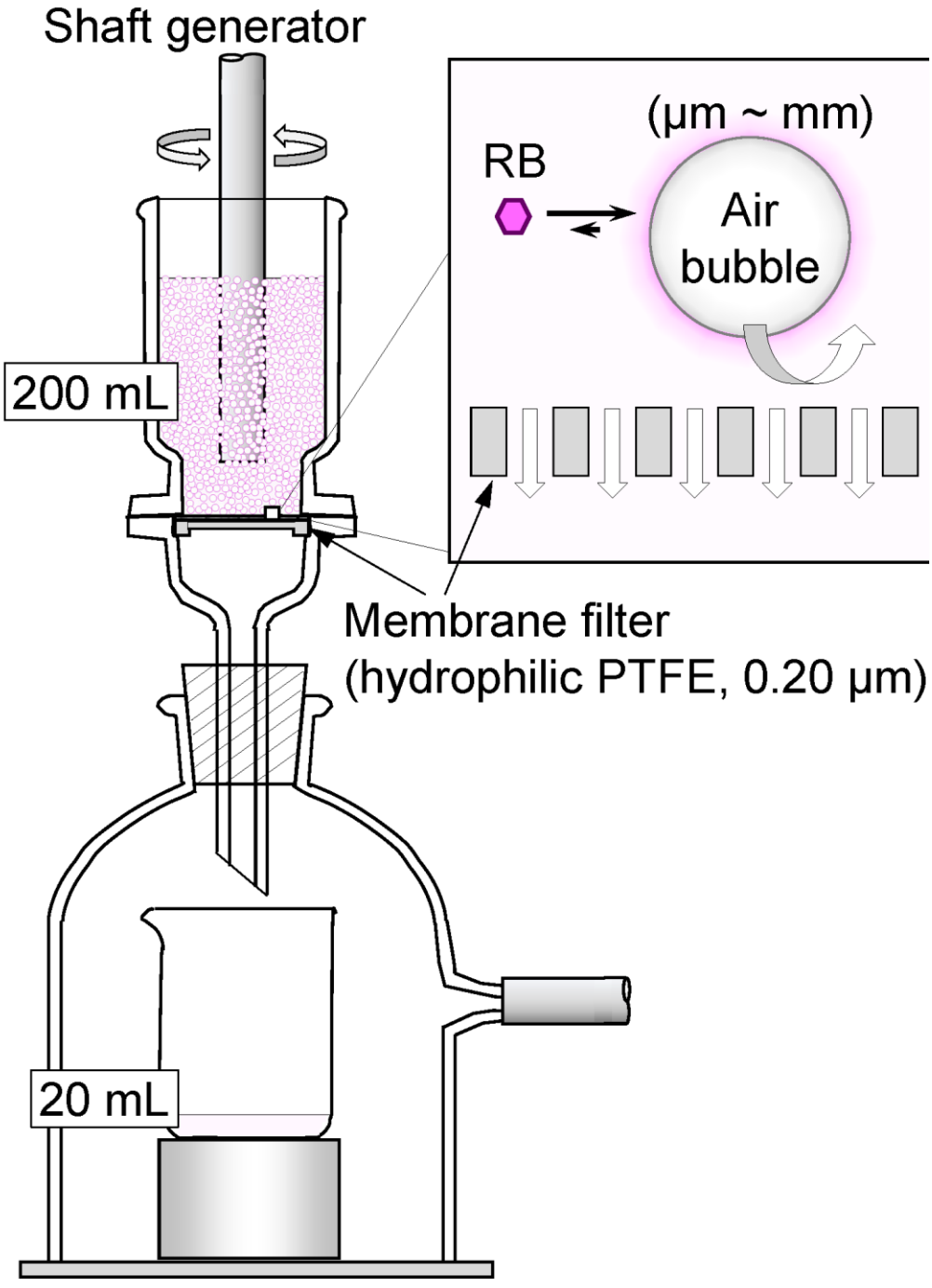

Fig. 4-1 Overview of air bubble-assisted membrane filtration.

4.2.3 Analysis of Air Bubbles

A Canon EOS 90D digital single-lens reflux camera (Tokyo, Japan) with an EF-S60mm F2.8 macro Ultra Sonic Motor single focus lens was used for taking photographs of air bubbles. The shutter speed was set to 1/8000 s. A couple of 50 W LED lamps were used for irradiating light to obtain high contrast images of air bubbles. The numbers of air bubbles having different size were countered by using an open source image processing software, Image J.

4.2.4 Dynamic Surface Tension Measurement

The dynamic surface tensions were measured with a DinoTester^{+} dynamic surface tensiometer (SITA Messtechnik GmbH, Dresden, Germany). Before experiments, all aqueous solutions were immersed in a water bath whose temperature was controlled at 25 ± 1°C with an EYELA CTP-1000 low temperature water circulator (Tokyo, Japan).

4.3 Results and discussion

When the shaft generator of the homogenizer was rotated at high speed, air was pulled into the aqueous solution and torn off to generate a large number of air bubbles. Fig.4-2 shows the effect of rotation speed of the shaft generator on the rejection ratio, R (%), of RB and MB.

$$R\,(\%) = \left(1 - \frac{C_f}{C_0}\right) \times 100 \quad \cdots \quad (1)$$

Here, C_0 denotes the initial concentration of a dye in the aqueous solution and C_f is the dye concentration in the filtrate solution. Both dyes were negligibly rejected when the rotation speed was lower than 8000 rpm. In this condition, no or few air bubbles were generated in the solution to be filtrate and hence the situation was the same as a normal membrane filtration. It is reasonable for these dye molecules (1.44 nm × 1.09 nm × 0.64 nm for RB [7] and 1.43 nm × 0.61 nm ×0.4 nm for MB [8]) much smaller than pore size (0.20 μm) to pass through the membrane filter. On the other hand, RB tended to be rejected above 8000 rpm of the rotation speed and the rejection ratio increased with increasing the rpm value. In the concentration of 2.0×10^{-6} to 2.0×10^{-5} mol dm^{-3}, the rejection ratio was almost independent of the concentration of RB. This indicates that the concentration, 5.0×10^{-6} mol dm^{-3}, of RB selected for obtaining accurate and precise results was lower than at which the effect of adsorption capacity of air bubbles is concern.

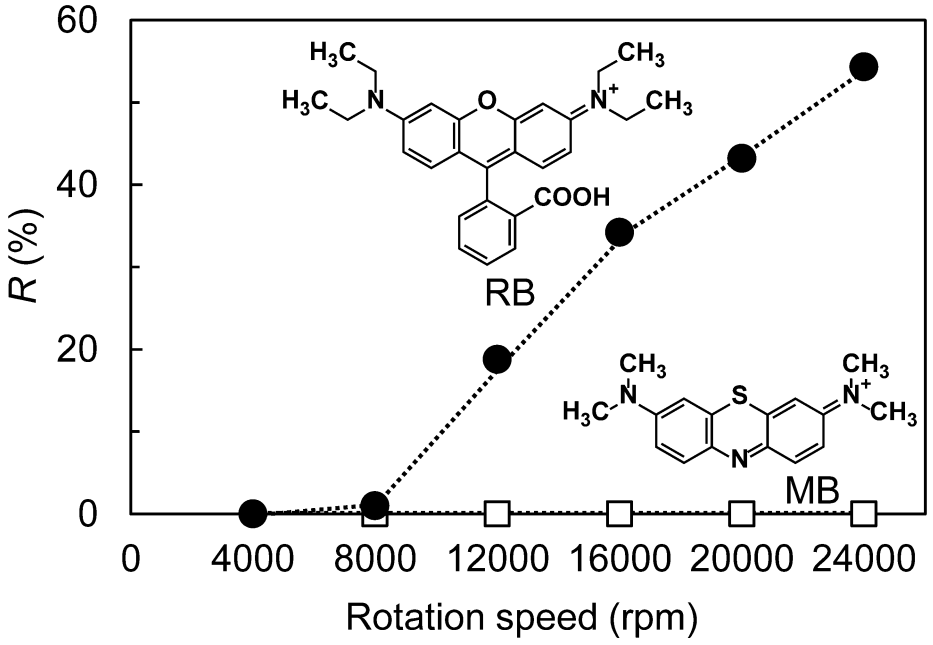

Fig. 4-2 Effect of rotation speed of a shaft generator of a homogenizer on the rejection ratio, R (%), of RB (filled circle) and MB (empty square). The model and type of the homogenizer and shaft genera tor are described in experimental section. 1-Butanol concentration: 0.05% (v/v)

Fig.4-3 shows the effect of 1-butanol concentration on the rejection ratios of RB and MB. In the absence of 1-butanol, RB was slightly rejected. On the other hand, the rejection ratio increased with increasing 1-butanol concentration. 1-Butanol is known as a weak frother which has often been used in flotation techniques to improve their separation efficiency [9,10]. It works to reduce the size of the air bubbles that are generated but is less effective in producing stable foam. As shown in the photo-pictures in Fig.4-3, the addition of 1-butanol significantly reduced the size of air bubbles. This result indicates the suitability of 1-butanol as an additive to reduce the size of air bubbles to increase the surface area of air bubbles for the adsorption of RB. However, the addition of further amount of 1-butanol resulted in the decrease in the rejection ratio of RB. 1-Butanol can adsorb on the air-water interface [11] and hence may suppress the adsorption of RB on the surface of air bubbles. Therefore, 1-butanol concentration was set to 0.05% (v/v) in the present study. Another basic dye, MB, was negligibly rejected under all conditions.

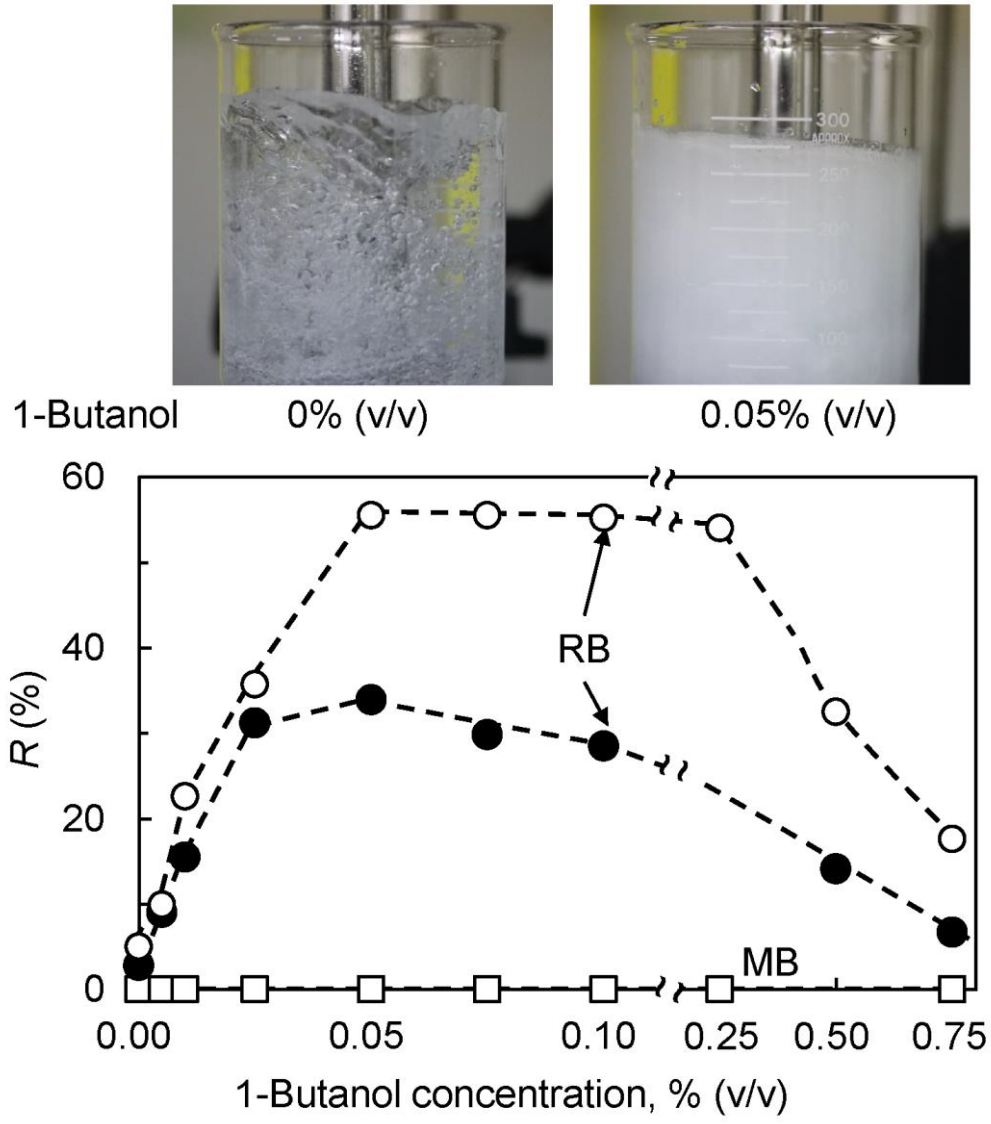

Fig. 4-3 Effect of 1-butanol concentration on the rejection ratio, R (%), of RB (filled circle, empty circle) and MB (empty square). Rota tion speed: (filled circle) 16,000 rpm, (empty circle, empty square) 24,000 rpm

Fig.4-4(A) lines up photo images of filtration funnels in which air bubbles are generated in the aqueous solution containing 0.05% (v/v) of 1-butanol by rotating a shaft generator of homogenizer at different rotation speed. As increasing the rotation speed, the solution became turbid due to the increased occurrence of fine air bubbles as well as inflated because of the increased amount of entrained air. Therefore, increased rejection of RB may be ascribable to the increasing surface area of air bubbles for the adsorption of RB. In the presence of 1-butanol, the shape of the air bubble was almost spherical regardless of their size. As a first approximation, the surface area, S_{est}, of air bubbles can be estimated from the product of the quantity of air bubble (n_i) having specified range of diameter (d_i) and the increase in solution volume (ΔV).

$$S_{est} = 4\pi \sum_i^m \left[\left(\frac{d_i}{2} \right)^2 \times n_i \right] \quad \cdot \cdot \cdot \quad (2)$$

$$\Delta V = \frac{4}{3}\pi \sum_i^m \left[\left(\frac{d_i}{2} \right)^3 \times n_i \right] \quad \cdot \cdot \cdot \quad (3)$$

The ΔV value meaning difference in the solution volumes with and without homogenizing the solution is attributed to the volume of generated air bubbles if their shapes are assumed to be spherical. Therefore, S_{est} value at each rotation speed was estimated from ΔV, d_i, and n_i. Fig.4-4(B) and 4(C) indicate an example of a set of particle analysis of air bubbles and their number-based size distribution. The correlation between rotation speed and estimated surface area of air bubbles, S_{est}, is shown in Fig. 4(D).

The effect of estimated surface area, S_{est}, of air bubbles on the rejection ratio, R(%), of two dyes is shown in Fig.4-5 whose horizontal axis is replaced from the rotation speed in Fig.4-2. The shape of the curve for RB seems a kind of adsorption isotherm, indicating that air bubbles play as adsorbents to control the membrane filtration.

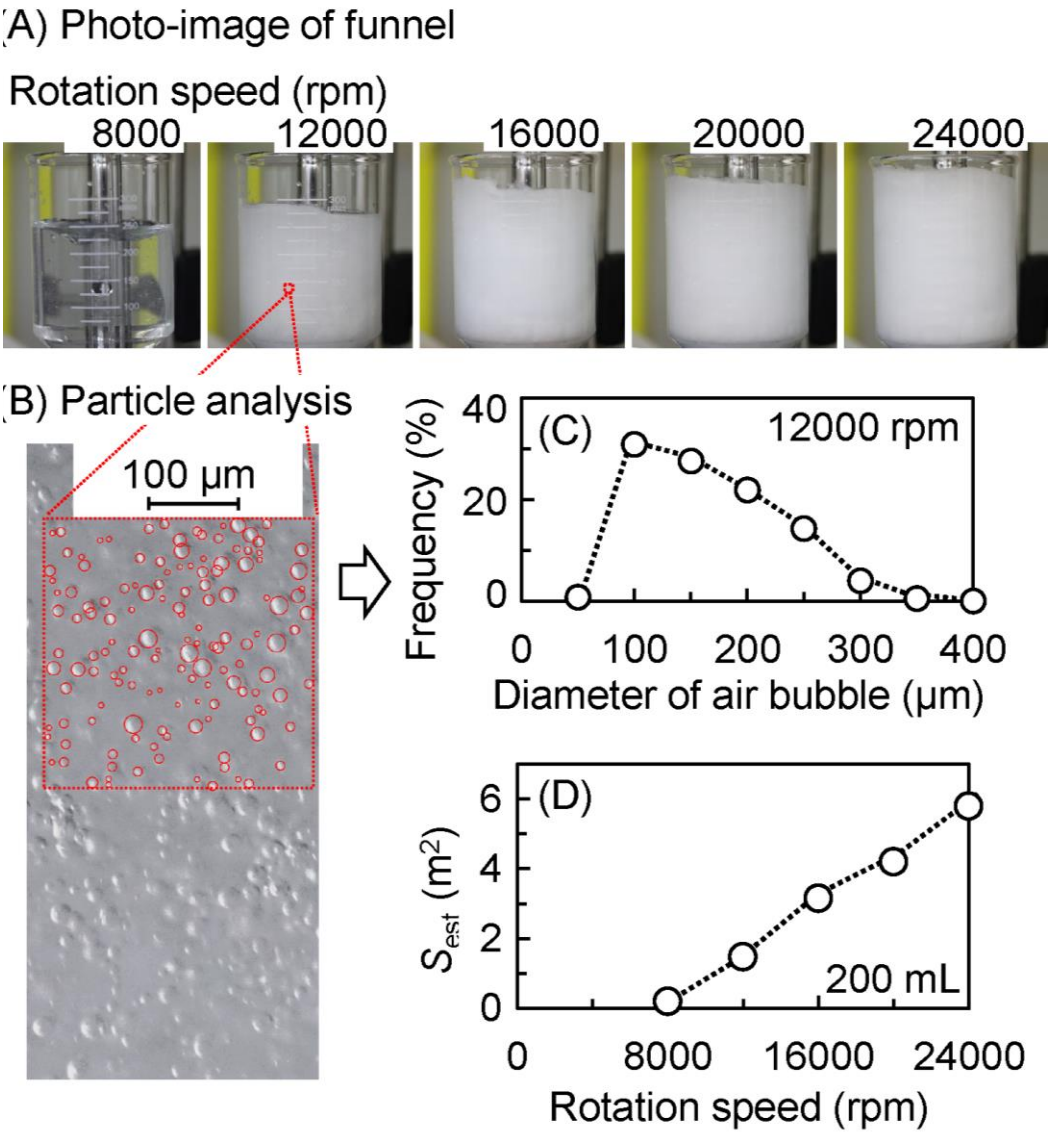

Fig.4-4 Photo images of separation funnels (A), an example set of par ticle analysis (B) and number-based size distribution of air bubbles (C), and estimated surface area of air bubbles, Sest, at different rota tion speeds (D). 1-Butanol concentration: 0.05% (v/v)

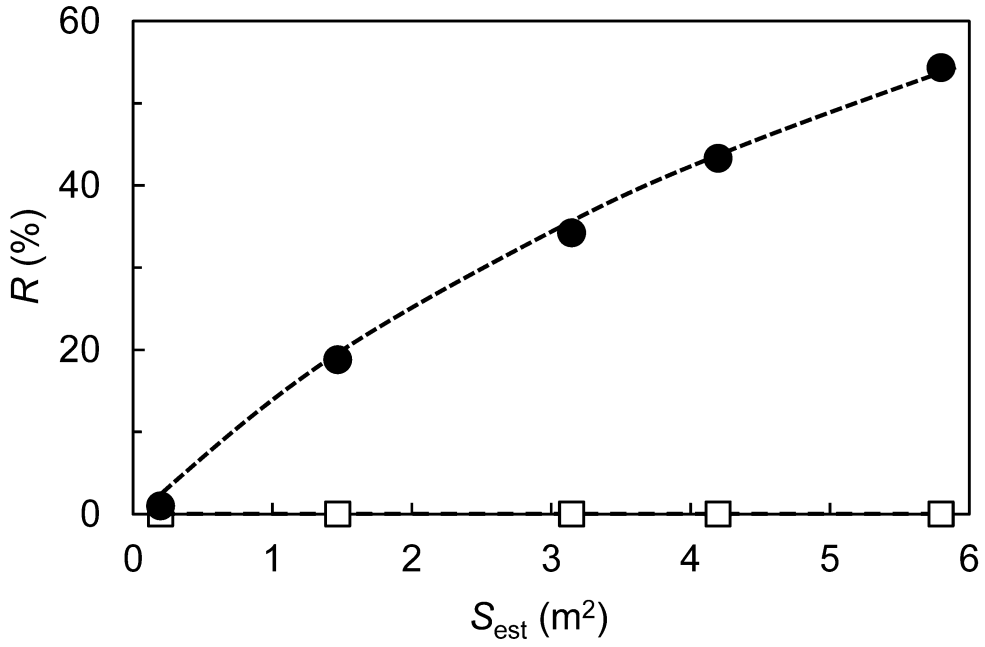

Fig. 4-5 Rejection ratio, R (%), of RB (filled circle) and MB (empty square) as a function of estimated surface area of air bubbles, S_{est}. 1-Butanol concentration: 0.05% (v/v)

As also shown in Fig.4-2, another dye, MB, was negligibly rejected even in the presence of lots of air bubbles (Fig.4-5). This is ascribable to very week adsorption of MB onto the surface of air bubbles. Strength of dye adsorption on the surface of air bubbles can be evaluated based on the effect of dye concentration on the surface tension of the aqueous solution. Fig.4-6 shows the dynamic surface tension of aqueous solution containing different amounts of RB or MB. The surface tension of RB solution significantly decreased with increasing the logarithmic concentration of RB, while the decrease in the surface tension of MB solution was very small. Large negative slope of the curve for RB having higher hydrophobicity (logarithmic aqueous-octanol distribution coefficient, log K_{ow} = 2.3 [12]) indicates strong adsorption of RB to the air-water interface. On the other hand, very small slope of the curve for MB indicates that MB having low hydrophobicity (log K_{ow} = 0.1 [13]) hardly adsorbs to the air-water interface. It is well-known that surfactant molecules having charged group and hydrophobic alkyl chain can strongly adsorb on the air-water interface [14-16] and the adsorption strength tend to increase with increasing the carbon number, therefore, hydrophobicity of the surfactant [17,18]. Resent molecular dynamic simulation studies clarified preferential distribution of inorganic ions such as iodide ions and amphiphilic organic molecules close to air-water interface [19]. These facts strongly support the adsorption of positively charged RB on the surface of air bubbles. The results obtained in the present study strongly suggest the possibility of selective membrane filtration dyes by utilizing the difference in adsorption strength on the surface of air bubbles.

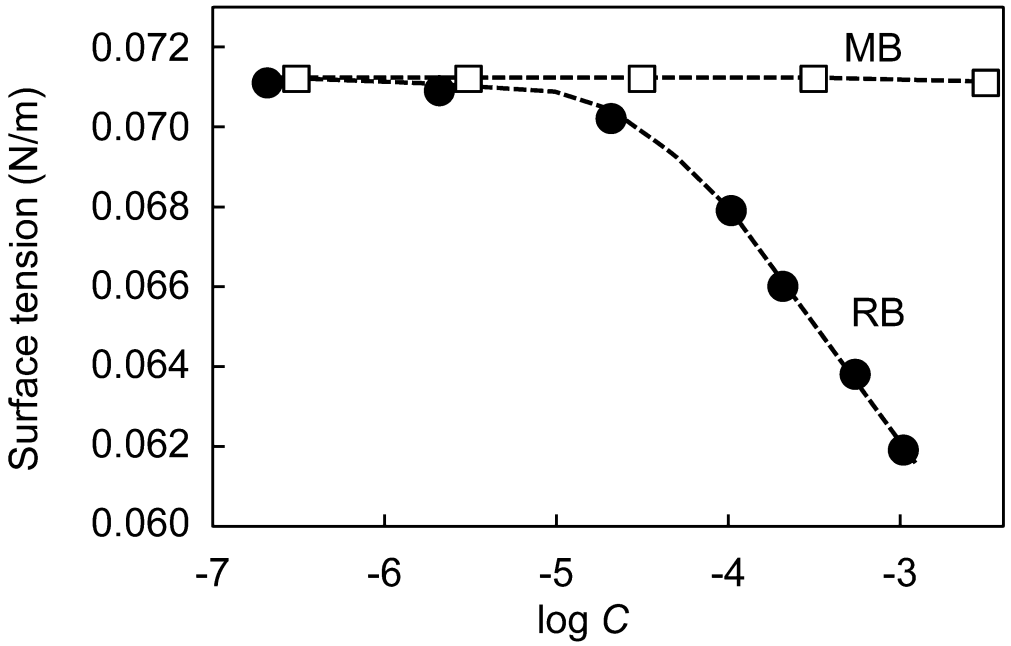

Fig.4-6 Dynamic surface tension of aqueous solution containing 0.05% (v/v) of 1-butanol and different amounts of RB (filled circle) or MB (empty square)

The proposed method may be compared with micellar enhanced ultrafiltration (MEUF), in which surfactant micelles being larger than the pore size of ultrafilter involve hydrophobic solutes and, therefore, enhance their rejection. MEUF processes have extensively been studied to remove different dissolved pollutants from wastewaters [21-23]. However, pressurization is necessary to operate ultrafiltration, because of small pore size of ultrafiltration membranes [22]. Moreover, the presence of highly concentrated surfactant hinders the recovery of useful components in the retentate solutions because of the difficulty in the elimination of the surfactant. On the other hand, the proposed method does not use surfactants or any additives that are difficult to remove. The filtration using membrane filters and other microfilters can be conducted by gravity-driven processes. The use of air bubbles may effective for selective separation of molecules or ions by microfiltration technique.

4.4 Conclusion of This Chapter

In the presence of air bubbles, RB ions were rejected by a hydrophilic PTFE membrane filter having 0.20 μm of pore diameter. The rejection ratio increased with increasing the amount of air bubbles in the RB solution to be filtrated. The rejection was explained by the adsorption of RB on the surface of air bubbles that hardly passed through the membrane filter. On the other hand, MB ions having lower hydrophobicity and, hence, having lower adsorption strength to air bubbles negligibly rejected. The results of the present study suggest the feasibility of the use of air bubbles as a kind of adsorbent for the selective microfiltration of molecules or ions.

4.5 References

[1]. A.W. Zularisam, A.F. Ismail, R. Salim, Behaviours of natural organic matter in membrane filtration for surface water treatment - a review, *Desalination*, **194**, 211–231 (2006). https://doi.org/10.1016/j.desal.2005.10.030

[2]. S Hube, M. Eskafi, K.F. Hrafnkelsdóttir, B. Bjarnadóttir, M.Á. Bjarnadóttir, S. Axelsdóttir, B. Wu, Direct membrane filtration for wastewater treatment and resource recovery: A review, *Sci. Total Environ*., **710**, 136375 (2020). https://doi.org/10.1016/j.scitotenv.2019.136375

[3]. W.J. Lau, A.F. Ismail, Polymeric nanofiltration membranes for textile dye wastewater treatment: preparation, performance evaluation, transport modelling, and fouling control - a review, *Desalination*, **245**, 321–348 (2009). https://doi.org/10.1016/j.desal.2007.12.058

[4]. A.W. Mohammad, Y.H. Teow, W.L. Ang, Y.T. Chung, D.L. Oatley-Radcliff, N. Hilal, Nanofiltration membranes review: Recent advances and future prospects, *Desalination*, **356**, 226–254 (2015). https://doi.org/10.1016/j.desal.2014.10.043

[5]. W. Pronk, A. Ding, E. Morgenroth, N. Derlon, P. Desmond, M. Burkhardt, B. Wu, A.G. Fane, Gravity-driven membrane filtration for water and wastewater treatment: A review, *Water Res*., **149**, 553–565 (2019). https://doi.org/10.1016/j.watres.2018.11.062 and references therein.

[6]. K. Kodama, M. Oiwa, T. Saitoh, Purification of Rhodamine B by alcohol-modified air bubble flotation, *Bull. Chem. Soc. Jpn.,* **94**, 1210–1214 (2021). https://doi.org/10.1246/bcsj.20200395

[7]. J.-H. Huang, K.-L. Huang, S.-Q. Liu, A-T. Wang, C. Yan, Adsorption of Rhodamine B and methyl orange on a hypercrosslinked polymeric adsorbent in aqueous solution, *Colloids Surf. A: Physicochem. Eng. Asp.*, **330**, 55–61 (2008). https://doi.org/10.1016/j.colsurfa.2008.07.050

[8]. C. Pelekani, V.L. Snoeyink, Competitive adsorption between atrazine and methylene blue on activated carbon: the importance of pore size distribution, *Carbon,* **38**, 1423–1436 (2000). https://doi.org/10.1016/S0008-6223(99)00261-4

[9]. Y. S. Cho, J. S. Laskowski, Effect of flotation frothers on bubble size and foam stability, *Int. J. Miner. Process*., **64**, 69−80, (2002). https://doi.org/10.1016/S0301-7516(01)00064-3

[10]. Y. S. Moreno, G. Bournival, S. Ata, Classification of flotation frothers – A statistical approach, *Chem. Eng. Sci.*, **248**, 117252 (2022). https://doi.org/10.1016/j.ces.2021.117252

[11]. P. Joos, G. Serrien, Adsorption kinetics of lower alkanols at the air, water interface: effects of structure maker, and structure breakers, *J. Colloid Inter. Sci*., **127**, 97−103 (1989). https://doi.org/10.1016/0021-9797(89)90010-6

[12]. L.F. Mottram, S. Forbes1, B.D. Ackley, B.R. Peterson, Hydrophobic analogues of rhodamine B and rhodamine 101: potent fluorescent probes of mitochondria in living *C. elegans*, *Beilstein J. Org. Chem.*, **8**, 2156–2165 (2012). https://doi.org/10.3762/bjoc.8.243

[13]. J.S. da Silva, H.C. Junqueira, T.L. Ferreira, Effect of pH and dye concentration on the n-octanol/water distribution ratio of phenothiazine dyes: a microelectrode voltammetry study, *Electrochim. Acta,* **144**, 154–160 (2014). https://doi.org/10.1016/j.electacta.2014.08.094

[14]. W. R. Gillap, N. D. Weiner, M. Gibaldi, Ideal behavior of sodium alkyl sulfates in various interfaces. Thermodynamics of adsorption at the air-water interface, *J. Phys. Chem*., **72**, 2218–2222, (1968). https://doi.org/10.1021/j100852a058

[15]. C.-H. Chang, E. I. Franses, Adsorption dynamics of surfactants at the air/water interface: a critical review of mathematical models, data, and mechanisms, *Colloid Surf. A Physicochem. Eng. Asp.*, **100**, 1–45 (1995). https://doi.org/10.1016/0927-7757(94)03061-4

[16]. A.J. Prosser, E.I. Franses, Adsorption and surface tension of ionic surfactants at the air–water interface: review and evaluation of equilibrium models, *Colloid Surf. A Physicochem. Eng. Asp.*, **178**, 1−40 (2001). https://doi.org/10.1016/S0927-7757(00)00706-8

[17]. A. Castro, K. Bhattacharyya, K. B. Eisenthal, Energetics of adsorption of neutral and charged molecules at the air/water interface by second harmonic generation: Hydrophobic and solvation effects, *J. Chem. Phys.*, **95**, 1310–1315 (1991). https://doi.org/10.1063/1.461113

[18]. T. Gilányi, I. Varga, C. Stubenrauch, R. Mészáros, Adsorption of alkyl trimethylammonium bromides at the air/water interface, *J. Colloid Interf. Sci*., **317**, 395–401 (2008).

[19]. P. Jungwirth, D. J. Tobias, Specific ion effects at the air/water interface, *Chem. Rev*., **106**, 1259–1281 (2006). https://doi.org/10.1021/cr0403741

[20]. D. Horinek, A. Herz, L. Vrbka, F. Sedlmeier, S. I. Mamatkulov, R. R. Netz, Specific ion adsorption at the air/water interface: The role of hydrophobic solvation, *Chem. Phys. Lett.*, **479**, 173–183 (2009). https://doi.org/10.1016/j.cplett.2009.07.077

[21]. R.O. Dunn Jr, J.F. Scamehorn, S.D. Christian, Use of micellar-enhanced ultrafiltration to remove dissolved organics from aqueous streams, *Sep. Sci. Technol*., **20**, 257–284 (1985). https://doi.org/10.1080/01496398508060679

[22]. M.K. Purkait, S. DasGupta, S. De, Removal of dye from wastewater using micellar-enhanced ultrafiltration and recovery of surfactant, *Sep. Sci. Technol*., **37**, 81–92 (2004). https://doi.org/10.1016/j.seppur.2003.08.005

[23]. M. Moreno, L.P. Mazur, S.E. Weschenfelder, R.J. Regis, R.A.F. de Souza, B.A. Marinho, A. da Silva, S.M.A.G.U. de Souza a, A.A.U. de Souza, Water and wastewater treatment by micellar enhanced ultrafiltration - A critical review, *J. Water Process Eng.,* **46**, 102574 (2022). https://doi.org/10.1016/j.jwpe.2022.102574

CHAPTER 5
CONCLUSION

The separation method using bubbles as a medium was shown to be an inexpensive, rapid, low environmental impact separation method and effective for the separation of drugs. This is thought to be due to the unique properties of bubbles, which act as a kind of solvent, selectively separating drugs.

In Chapter 2, the microscopic solvent properties of bubbles (air-water interface) were evaluated by fluorescence analysis using 1,2`-dinaphthylamine, a fluorescent molecule. Its fluorescence spectrum fluctuated with the presence of bubbles, with the λ_{max} values shifting from 486 nm to 408 nm, toward the shorter wavelength side, suggesting the presence of hydrophobic fields on the bubble surface. Compared to the fluorescence spectra of generic solvents, the bubbles showed λ_{max} values similar to those of ethyl acetate (416 nm) and diethyl ether (406 nm). This shows one aspect of air bubbles as an inexpensive green solvent.

In Chapter 3, it was revealed that with a thorough understanding of the properties of bubbles and the right conditions, the purification of chloroquine can be accomplished in 10 minutes. It was found that the highly hydrophobic non-ionic form of chloroquine interacted most strongly with bubbles and was well adsorbed to bubbles under strong alkaline conditions at pH 12. On the other hand, the less hydrophobic source materials were not strongly adsorbed onto the bubbles under any conditions. It was suggested that separation using bubbles is affected by the hydrophobicity (log K_{ow}) and ionic properties of the compound. The developed method was better than conventional methods because it avoids the use of highly toxic organic solvents and requires fewer steps, making it a separation method for green chemistry.

In Chapter 4, we discussed the possibility of using this technology in combination

with microfiltration to achieve even higher speeds and continuous processing. The separation time was further accelerated to less than one minute, suggesting the possibility of larger equipment and application to continuous processing, which would be effective in industrial production.

Air bubbles were an easy to generate, inexpensive and harmless separation medium. In addition, adsorption of molecules onto bubbles was extremely rapid. The drug separation technology using bubbles as a medium developed in this study was expected to contribute to sustainable industry as a new separation and purification method in the chemical industry.

Acknowledgment

I would like to express my sincere gratitude to my advisor, Professor Tohru Saitoh[1] for him thoughtful guidance. I am also particularly grateful to Dr. Hideo Hayashi[2] and Associate Professor Keiji Yasuda[3] for their continuous support.

1. Graduate School of Engineering, Kitami Institute of Technology, 165 Koen-Cho, Kitami, Hokkaido 090-8507, Japan.
2. Tokyo Metropolitan Industrial Technology Research Institute, Aomi 2-4-10, Koto-ku, Tokyo 135-0064, Japan.
3. Graduate School of Engineering, Nagoya University, Furo-Cho, Chikusa-Ku, Nagoya, Aichi 464-8603, Japan.